

AD A11 3030

AD-F 300 010

AD

TECHNICAL REPORT ARBRL-TR-02390

EXPLOSIVE DRIVER APPLICATION FEASIBILITY
STUDY AND TEST FOR USE IN THE
HYPERVELOCITY LAUNCH OF
HIGH DENSITY HIGH L/D
PROJECTILES

Evan Harris Walker

STIC
ELECTE
APR 2 1982
A

February 1982



US ARMY ARMAMENT RESEARCH AND DEVELOPMENT COMMAND
BALLISTIC RESEARCH LABORATORY
ABERDEEN PROVING GROUND, MARYLAND

Approved for public release; distribution unlimited.

DTIC FILE COPY

82 02 06 012

Destroy this report when it is no longer needed.
Do not return it to the originator.

Secondary distribution of this report by originating
or sponsoring activity is prohibited.

Additional copies of this report may be obtained
from the National Technical Information Service,
U.S. Department of Commerce, Springfield, Virginia
22161.

Accession For	
NTIS GRA&I	<input checked="checked" type="checkbox"/>
DTIC TAB	<input type="checkbox"/>
Unannounced	<input type="checkbox"/>
Justification	
By _____	
Distribution/	
Availability Codes	
Date	or
A	



The findings in this report are not to be construed as
an official Department of the Army position, unless
so designated by other authorized documents.

*The use of trade names or manufacturers' names in this report
does not constitute endorsement of any commercial product.*

UNCLASSIFIED

SECURITY CLASSIFICATION OF THIS PAGE (When Data Entered)

REPORT DOCUMENTATION PAGE		READ INSTRUCTIONS BEFORE COMPLETING FORM
1. REPORT NUMBER Technical Report ARBRL-TR-02390	2. GOVT ACCESSION NO. AD-A113 030	3. RECIPIENT'S CATALOG NUMBER
4. TITLE (and Subtitle) EXPLOSIVE DRIVER APPLICATION FEASIBILITY STUDY AND TEST FOR USE IN THE HYPER- VELOCITY LAUNCH OF HIGH DENSITY HIGH L/D PROJECTILES		5. TYPE OF REPORT & PERIOD COVERED Final
7. AUTHOR(s) Evan Harris Walker		6. PERFORMING ORG. REPORT NUMBER
9. PERFORMING ORGANIZATION NAME AND ADDRESS US Army Ballistic Research Laboratory (ATTN: DRDAR-BLT) Aberdeen Proving Ground, MD 21005		8. CONTRACT OR GRANT NUMBER(s)
11. CONTROLLING OFFICE NAME AND ADDRESS US Army Armament Research and Development Command US Army Ballistic Research Laboratory (ATTN: DRDAR-BL) Aberdeen Proving Ground, MD 21005		10. PROGRAM ELEMENT, PROJECT, TASK AREA & WORK UNIT NUMBERS 1L161102AH43
14. MONITORING AGENCY NAME & ADDRESS (if different from Controlling Office)		12. REPORT DATE FEBRUARY 1982
		13. NUMBER OF PAGES 52
		15. SECURITY CLASS. (of this report) UNCLASSIFIED
		15a. DECLASSIFICATION/DOWNGRADING SCHEDULE
16. DISTRIBUTION STATEMENT (of this Report) Approved for public release, distribution unlimited.		
17. DISTRIBUTION STATEMENT (of the abstract entered in Block 20, if different from Report)		
18. SUPPLEMENTARY NOTES		
19. KEY WORDS (Continue on reverse side if necessary and identify by block number) Hypervelocity Gun Explosive Driver Muzzle Accelerator		
20. ABSTRACT (Continue on reverse side if necessary and identify by block number) (kjm) A study of explosive drivers for use in short term experimental ballistics programs requiring hypervelocity launch capability for high density, high L/D projectiles has been carried out. The study focused on the problems associated with the application of explosive drivers as a possible simple expedient in ballistics programs requiring a small number of test shots. Since prior use of explosive drivers has not dealt with the launch of high density, high L/D projectiles, the study concentrated on problems associated with the (continued)		

DD FORM 1 JAN 73 1473

EDITION OF 1 NOV 65 IS OBSOLETE

UNCLASSIFIED

SECURITY CLASSIFICATION OF THIS PAGE (When Data Entered)

UNCLASSIFIED

SECURITY CLASSIFICATION OF THIS PAGE(When Data Entered)

redesign of explosive drivers for ballistics applications. The study pinpointed several problem areas, specifically radiative heat loss to the gas reservoir and bore walls, projectile stability (at high L/D) during high pressure launch and the well recognized problems associated with chamber block - gas reservoir closure and integrity.

The equations prescribing the design of an explosive driver gun have been derived for the general case in which driver length constraints may exist based on the projectile and velocity requirements, as well as pressure loading limits on the projectile. These equations show that it is very difficult to meet the restrictions imposed by hypervelocity accelerators employing explosive drivers to launch high density, high L/D projectiles.

A specific device was designed and fabricated for a 0.281 inch (0.7137 cm) diameter 6.3634 g steel projectile to achieve 6.24 km/s. Break wires and flash x-ray equipment were provided for instrumentation. Projectile integrity was not maintained during launch. It appears that extensive additional effort would be required to achieve successful hypervelocity launches of high density, high L/D projectiles with explosive drivers without resorting to far larger devices to provide large sabots for the projectiles.

UNCLASSIFIED

SECURITY CLASSIFICATION OF THIS PAGE(When Data Entered)

TABLE OF CONTENTS

	Page
LIST OF ILLUSTRATIONS	5
LIST OF TABLES	7
I. INTRODUCTION	9
II. EXPLOSIVE DRIVER GUNS	11
III. PRESSURE TUBE DIMENSIONS	16
IV. RELATION BETWEEN GAS RESERVOIR AND LAUNCH VELOCITY	20
V. LOADING PRESSURE IN THE GAS PRESSURE TUBE	22
VI. COMPUTED DESIGN: 1/2" CALIBER, 1/4" CALIBER AS TESTED	24
VII. HIGH EXPLOSIVE INDUCED BARREL CLOSURE	31
VIII. SELECTION OF MATERIALS	33
IX. TEST SETUP, PROCEDURE, AND DIAGNOSTICS	38
X. TEST RESULTS	45
XI. CONCLUSIONS	46
REFERENCES	49
DISTRIBUTION LIST	51

LIST OF ILLUSTRATIONS

Figure	Page
1. Explosive Driver Gun.	10
2. Schematic of an explosive driver section	12
3. Density ρ , pressure p and sound velocities a in the shocked and unshocked pressure tube gas. Also shown is the detonation wave having velocity D and shock wave at velocity S	14
4. Illustration of successive stages in the collapse of the pressure tube	15
5. Diagram of (a) explosive driver gun illustrating dimensions important to gun design and (b) $x - t$ plot of piston and shock wave as related to pressure tube dimensions.	17
6. Design performance curves for reservoir gun, after Seigel ⁷ , $\gamma = 5/3$, $d_0/d_1 = 5$	21
7. Design of the explosive driver gun, projectile and sabot as fabricated	30
8. Plot of calculated earliest time of arrival for shock as a function of bore position.	32
9. Photograph of the test chamber block used to determine adequacy of the breech bevel ring dimensions.	34
10. Absorptance (ratio of absorbed to incident energies) for pure aluminum as function of photon energy.	36
11. Reflectance of photons for aluminum as function of energy	37
12. Fixture to hold baratol tube, vacuum line hookup, break wires, x-ray "windows," and projectile exit "window," as tested	39
13. Photograph of explosive driver gun as tested mounted on a table with the explosive driver	41
14. Photograph of the explosive driver and chamber block.	42

LIST OF ILLUSTRATIONS (continued)

Figure		Page
15.	Photograph of the muzzle accelerator device and velocity "screens"(break wire fixtures).	43
16.	Photograph of the explosive driver gun looking down the length of the device.	44
17.	End of barrel attached to chamber block as recovered. (A) End view showing conical plug of sheared steel from the chamber block and the enlarged bore. (B) Side view.	47

LIST OF TABLES

Number	Page
I. Computed and As Tested Driver Design.25
II. Values of u_p , projectile muzzle velocity, for choices of G/M_p , ratio of gas (reservoir) to projectile mass, for $\bar{x} = 0.325$ and $d_0/d_1 = 5$27
III. Computed and Fabricated Design Parameters28

I. INTRODUCTION

The Explosive Driver is a device invented at Physics International capable of generating a high temperature, high density light (low molecular weight) gas (generally helium).¹⁻⁶ The resulting reservoir of gas can be used to accelerate projectiles in an attached launch tube. A schematic of an explosive driver hypervelocity gun is shown in Figure 1. Such devices have been used at Physics International to achieve launch of projectiles weighing 2.36 kg to a velocity of 6.5 km/sec, 11.5 kg to 3.2 km/sec (the "Alpha I shot"; early pressure chamber failure prevented achievement of the 5.5 km/sec design velocity), and in a modified two stage driver⁵, 2g to 12.0 km/sec.

Explosive driver devices are basically simple and inexpensive. They are far smaller than light gas gun facilities of the same projectile mass and velocity capability, lending themselves to the task of conducting hypervelocity tests without the need for maintaining a large light gas gun facility.

On the other hand, the explosive drivers are good for only one shot with little salvagable (for ordinary explosive driver designs). Successful use of explosive drivers for projectile launch has been achieved only for projectile having an L/D of about 1 (Physics International Company practice has been to use $L/D = 0.8$ in many cases.) Projectile density has also been low (Physics International Company has used such materials as polyethylene, polycarbonate³, and a Lithium-Magnesium alloy achieving a density of 1.38 g/cm^3).

¹J. D. Watson, E. T. Moore, Jr., D. Mumma, and J. S. Marshall, "Explosively-Driven Light Gas Guns", PIFR - 024/065, Physics International Company, San Leandro, CA, Sep 67.

²E. T. Moore, Jr., "Explosive Hypervelocity Launchers", NASA CR - 982, National Aeronautics and Space Administration, Feb, 68.

³J. D. Watson, "An Explosively Driven Gun to Launch Large Models to Re-entry Velocities," PIFR - 098, Physics International Company, San Leandro, CA, Apr, 69.

⁴J. D. Watson, "High Velocity Explosively Driven Guns," PIFR - 113, Physics International Company, San Leandro, CA, Jul, 69.

⁵J. D. Watson, "A Summary of the Development of Large Explosive Guns for Re-entry Simulation," PIFR - 155, Physics International Company, San Leandro, CA, Aug, 70.

⁶E. T. Moore, Jr., "Explosive Hypervelocity Launchers", PIFR - 051, Physics International Company, San Leandro, CA, Sep, 76.

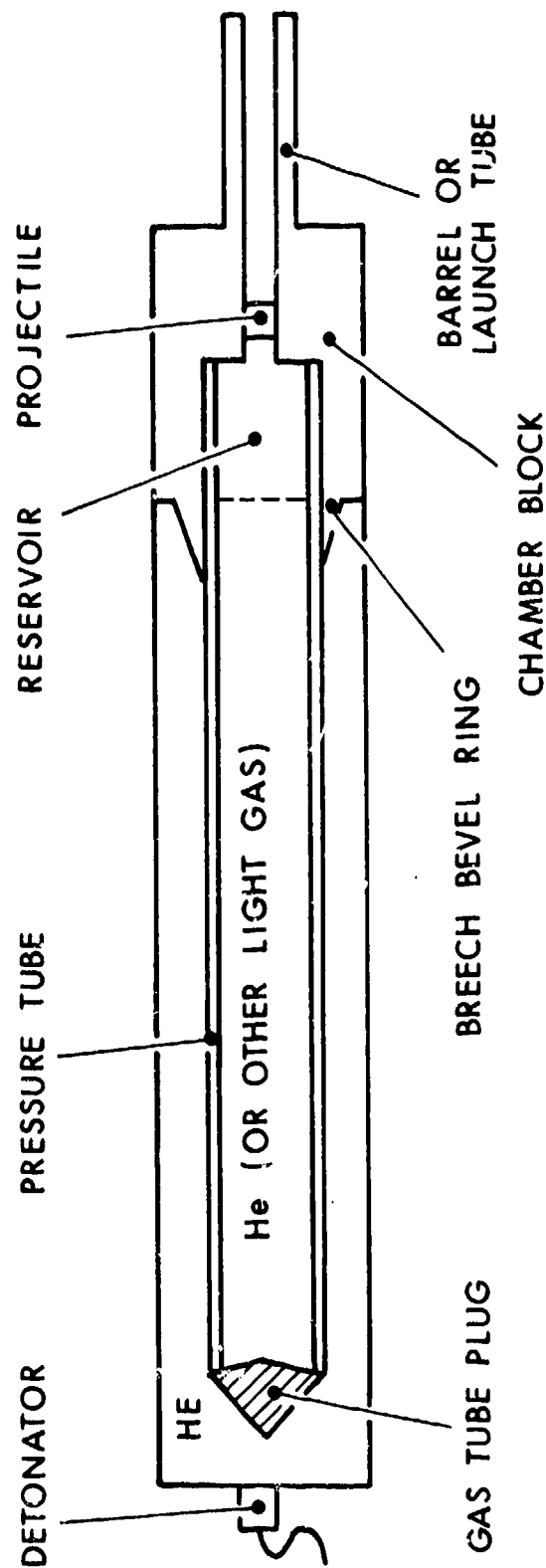


Figure 1 - Explosive Driver Gun. Initiation of one detonator produces a detonation wave that travels down the high explosive (HE) "tube" collapsing the pressure tube containing a light gas, usually helium (He). The reservoir, to contain the resulting high pressure, high temperature gas, is formed in the section of the pressure tube forward of the dashed line when the breech bevel ring is closed by the HE. The reservoir gas then propels the projectile through the barrel.

Since the explosive driver could serve as a valuable tool in BRL research to provide hypervelocity tests in programs that otherwise do not justify the expense of light gas gun facilities, a limited in-house effort was undertaken to determine if explosive drivers could be advantageously employed in typical test programs of interest at BRL. The program has been tied to a separate test, an in-house program on a muzzle accelerator device requiring the launch of a steel projectile with $L/D = 6$ to a velocity of 5 to 6 km/sec. Details of the muzzle accelerator program are given in a separate report. The exact projectile description is detailed below.

II. EXPLOSIVE DRIVER GUNS

A diagram of an explosive driver as applied to projectile launch is shown in Figure 1. Initiation of the detonator gives rise to a detonation front collapsing the pressure tube (see also Figure 4), and driving a shock wave down the length of the pressure tube. A ramp-like breech bevel ring on the chamber block is closed by the high explosive (HE), just as the reflected shock arrives at the rear of the reservoir (indicated by the dashed line in Figure 1). The high pressure gas contained in the reservoir thus formed accelerates the projectile through the launch tube.

Details for the design of optimum explosive drivers have been given by Watson.⁴ Here optimum is defined in terms of the use of the overall driver mass to produce a given reservoir. This design results in a rather long device (the pressure tube alone turns out to be 30 diameters ID in length). For many applications overall length can be an important consideration, particularly, if as in the present program, cast HE is employed, rather than a liquid explosive as has been the Physics International Company practice, since for large devices this results in handling problems for the HE loading. Figure 2 shows schematically the manner in which detonation of the HE in an explosive driver produces a volume of shock heated and compressed gas. For reference, the explosive driver gun is shown before, Figure 2a, as well as after the detonation wave has propagated some distance along the tube, Figure 2b. As the detonation front passes a section of the pressure tube, the pressure tube is collapsed into a conical rear surface. Although the material forming the rear surface of this tube collapses radially to form the "collapsed pressure tube" indicated in Figure 2b, the rear surface forms a constant geometry conical piston that drives forward, shock heats, and compresses the pressure tube gas. This piston moves at the detonation velocity D . The resulting shock front moves out ahead of this piston at a velocity S as given for ideal gases by⁵

$$S = \frac{1}{2} (\gamma + 1) D \quad (1)$$

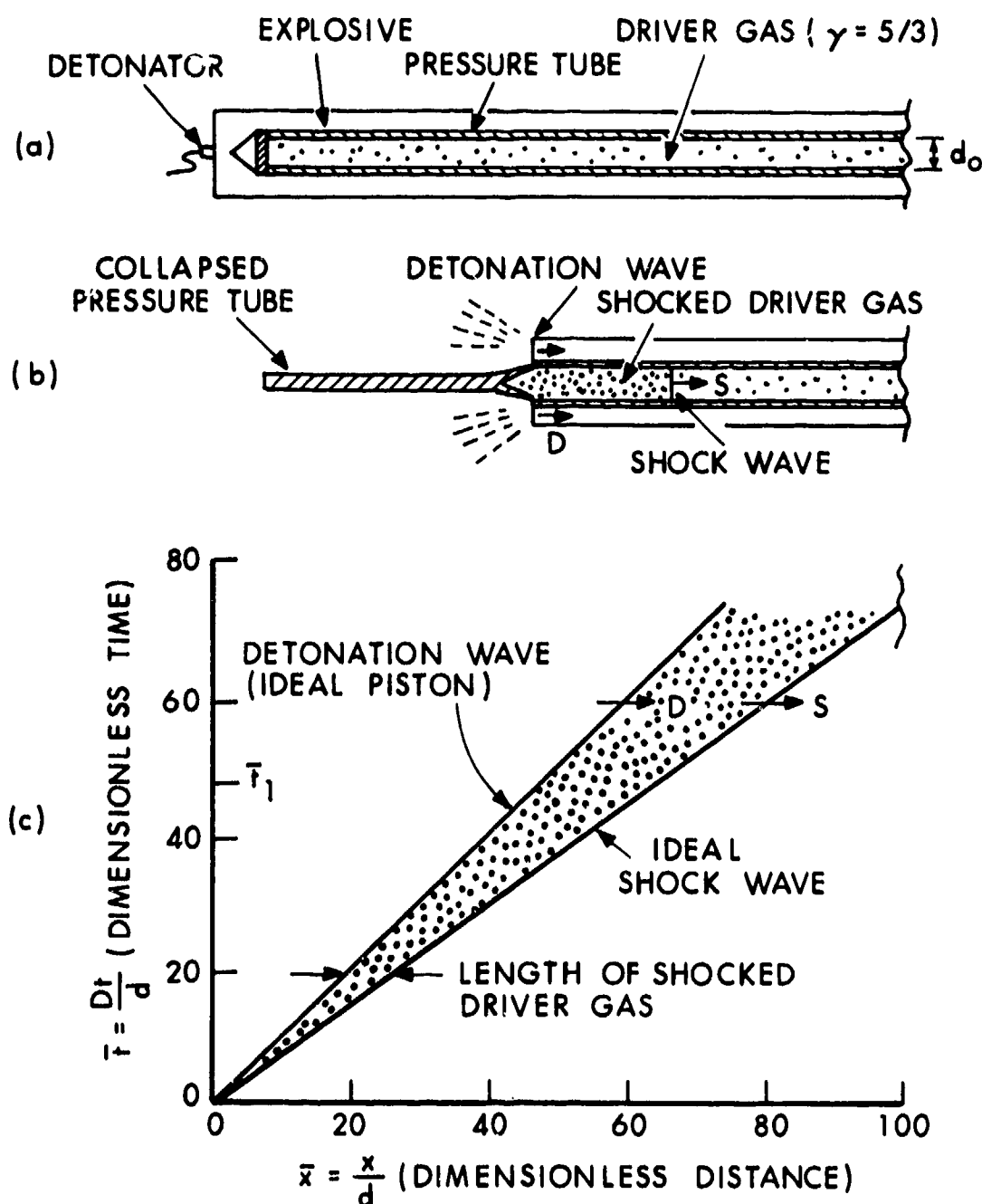


Figure 2 - Schematic of an explosive driver section (a) before and (b) after initiation of the detonation; (c) resulting distance vs. time plot of ideal explosive driver piston and shock wave. Length of shocked driver gas column at any time is also shown.

where γ is the ratio of specific heats in the pressure tube gas. In most cases the optimum⁷ gas to use in such devices is helium since its molecular weight is low and it has a high value of γ ($= 5/3$), both contributing to increased projectile velocity. Detonation front (approximate piston position) and shock front positions as a function of time are shown for the ideal driver in Figure 2c.

For an ideal gas in the pressure tube having density ρ_1 , and sound velocity a_1 (see Figure 3) passage of the shock front moving with velocity S as given by Equation (1) yields density ρ_2 and sound velocity a_2 after shock passage⁸ where:

$$\rho_2 = \rho_1 \frac{\gamma + 1}{\gamma - 1} \quad (2)$$

$$p_2 = \frac{1}{2} (\gamma + 1) \rho_1 D^2 = p_1 (\gamma + 1) D^2 / 2RT \quad (3)$$

and

$$a_2 = \sqrt{\frac{1}{2} \gamma (\gamma - 1) D} \quad (4)$$

as is readily obtained from the ideal gas laws and conservation laws for shock gas. The temperature before and after shock passage, T_1 and T_2 respectively are related by⁸

$$T_2 = T_1 \rho_1 p_2 / \rho_2 p_1 \quad (5)$$

When the shock front reaches the end of the pressure tube, it reflects off the relatively massive chamber block as shown in Figure 4, producing additional shock heating of the reservoir gas. The final pressure, p_4 , in the gas reservoir that is formed when the chamber closes is given by^{7,8}

$$p_4 = p_2 \left(2 + \frac{\gamma + 1}{\gamma - 1} \right) \quad (6)$$

at a density ρ_4 given by

$$\rho_4 = \rho_2 \gamma (\gamma + 1) \quad (7)$$

⁷A. E. Seigel, *The Theory of High Speed Guns*, published by North Atlantic Treaty Organization: AGARD ograph - 91. Reproduced by National Technical Information Service, Springfield, VA 22151, May 65.

⁸R. Von Mises, *Mathematical Theory of Compressible Fluid Flow*, Academic Press, 1958.

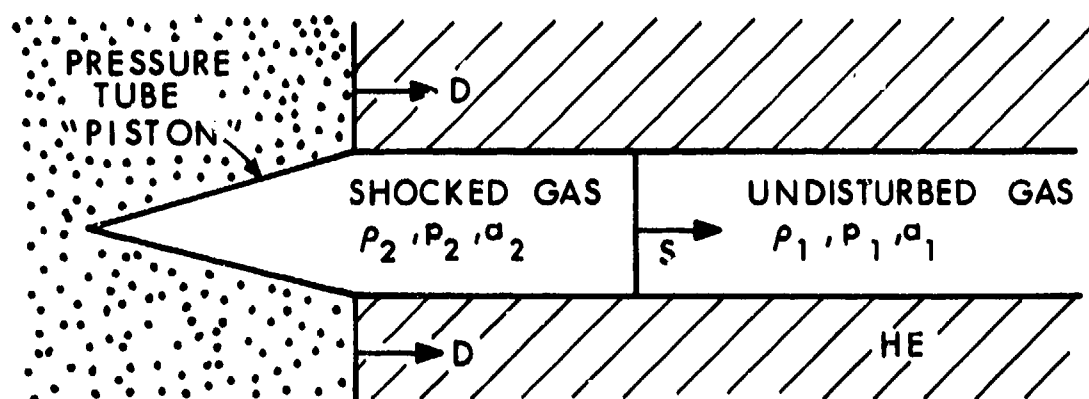


Figure 3 - Density ρ , pressure p and sound velocities a in the shocked and unshocked pressure tube gas are important in the description of driver functioning. Also shown is the detonation wave having velocity D and shock wave at velocity S .

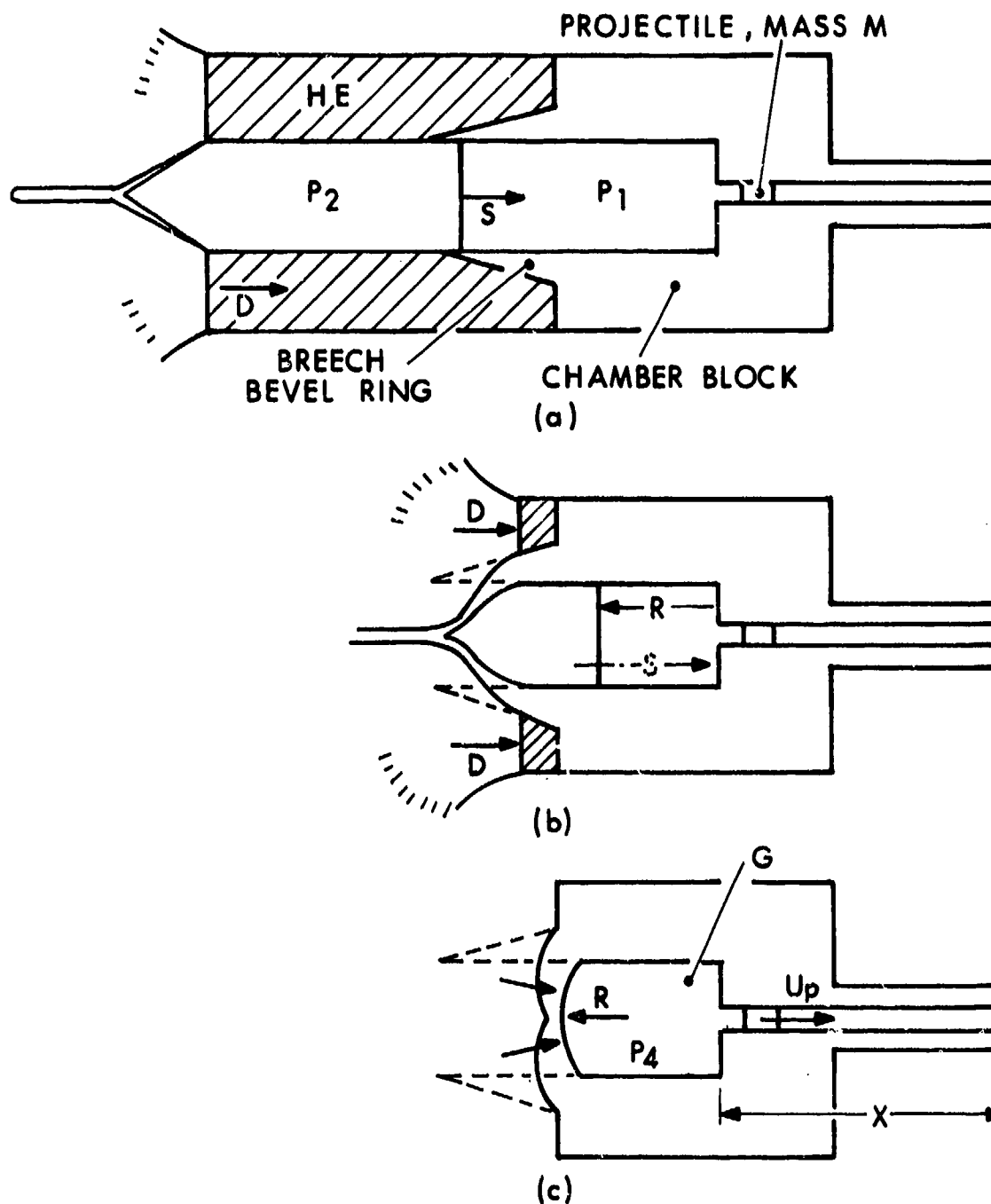


Figure 4 - (a) Illustration of successive stages in the collapse of the pressure tube, (b) closure of the breech bevel ring, and (c) formation of the gas reservoir of mass G and pressure P_4 in the chamber block as the reflected shock R meets the closed breech.

The sound velocity a_4 and reflected shock velocity R are given by^{7,8}

$$a_4 = \left[\frac{1}{2} (3\gamma - 1) (\gamma - 1) \right]^{1/2} D \quad (8)$$

and

$$R = 2 \left(\frac{\gamma - 1}{\gamma + 1} \right) S \quad (9)$$

The reflected shock brings the gas to rest just as the chamber closes, as shown in Figure 4, so that all the shocked gas is enclosed. In addition to the above equations for the reservoir gas pressure, density and sound velocity, one must also specify the dimensions of the gun and projectile together with the projectile mass to determine the launch velocity for the device.

III. PRESSURE TUBE DIMENSIONS

Let us now consider the factors that determine the dimensions of a pressure tube. Figure 2c gives an overly idealized representation of the shock in the pressure tube. Experiments with explosive drivers conducted by the Physics International Company¹⁻⁶ show that the shock does not immediately break out ahead of the detonation front as indicated by Figure 2c. Instead a distance equal to 4 tube diameters has been found to be required for shock break out to occur. Indicating this distance by L_s and the tube diameter by d_0 , we have

$$L_s = 4d_0 \quad (10)$$

Break out of the shock is illustrated in Figure 5. Some important dimensions of the explosive driver gun are also defined in Figure 5a. In addition, the shock reflects off the front of the pressure tube at a value of x , as in Figure 5, equal to the length L of the pressure tube where

$$L = L_s + L_g + L_R \quad (11)$$

The quantities L_g and L_R being defined by the illustration Figure 5a.

At the time the shock reflects off the front of the chamber block, the detonation front is at a distance L' behind the shock, where

$$L' = L_g + L_R - D(L_g + L_R)/S \quad (12)$$

since

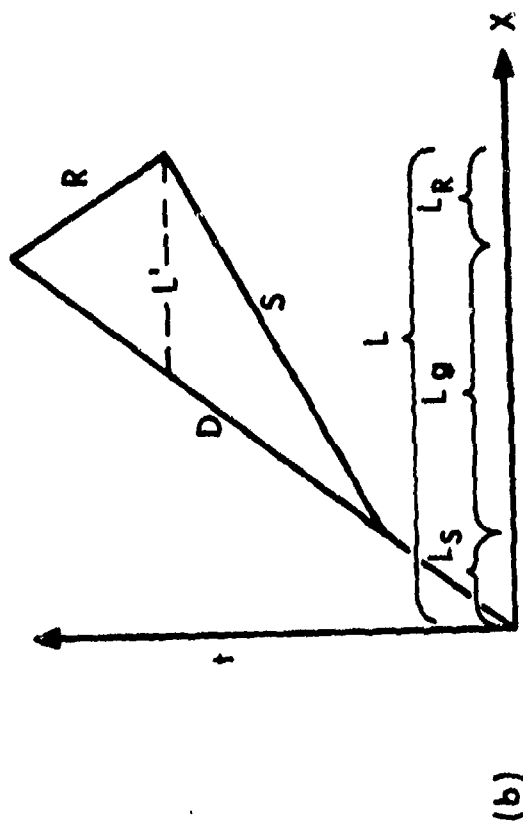
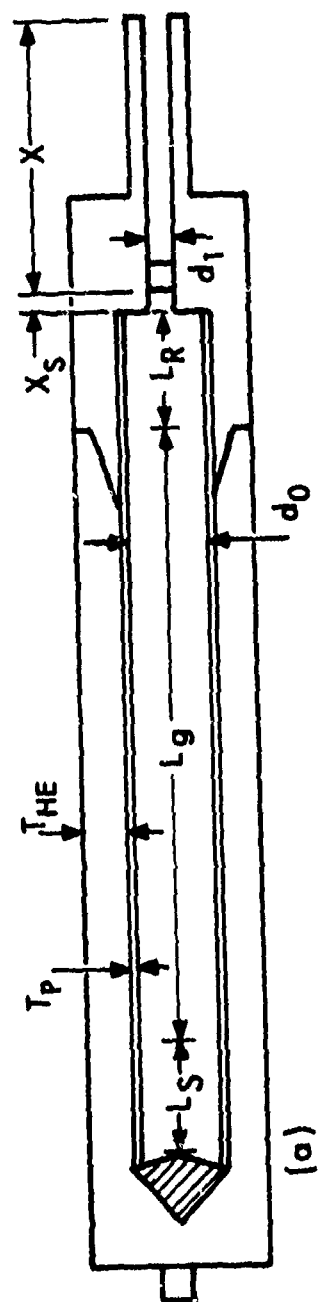


Figure 5 - Diagram of (a) explosive driver gun illustrating dimensions important to gun design and (b) $x - t$ plot of piston and shock wave as related to pressure tube dimensions.

$$S = \frac{1}{2} (\gamma + 1) D \quad (13)$$

Equation (12) becomes

$$L' = (L_g + L_R) \left(1 - \frac{2}{\gamma + 1}\right) \quad (14)$$

The reservoir length L_R is given by the condition that the detonation front arrives at the rear face of the reservoir at the same time the reflected shock arrives there. Therefore we have

$$L_R/R = (L' - L_g)/D \quad (15)$$

Substituting in Equation (15) for L' from Equation (14) gives

$$L_R = L_g (\gamma - 1)^2 / (3\gamma - 1) \quad (16)$$

or for $\gamma = 5/3$

$$L_R = L_g / 9 \quad (17)$$

The overall length of the pressure tube is, therefore,

$$L = 4d_0 + [1 + (\gamma - 1)^2 / (3\gamma - 1)] L_g \quad (18)$$

and again, for $\gamma = 5/3$ this becomes

$$L = 4d_0 + \frac{10}{9} L_g \quad (19)$$

or in terms of a desired reservoir length

$$L = 4d_0 + 10L_R \quad (20)$$

Experimental tests of explosive drivers at Physics International Company have yielded a maximum effective value for L' . Energy loss to the pressure tube walls (for example, due to viscous losses) are such that the shock does not run more than about 6 tube diameters ahead of the detonation front. Thus, L' is limited according to

$$L' \leq 6d_0 \quad (21)$$

If L' is set equal to $6d_0$, an optimum design is obtained. In this case one obtains for this optimum length L_{opt} of the explosive driver pressure tube

$$L_{opt} = 2d_0 \left(\frac{5\gamma + 1}{\gamma - 1} \right) \quad (22)$$

and for $\gamma = 5/3$,

$$L_{opt} = 28d_0 \quad (23)$$

Physics International Company practice has been to round off this figure and use $L = 30d_0$ which has worked well.

Unfortunately, such lengths can be inconvercent in large caliber devices. This is of particular concern if cast explosive is to be used in the driver. For example, a 0.1016 m diameter pressure tube would be 3.048 m in length and pose additional difficulties to the explosive Hot Melt facility at BRL. Such difficulties are not encountered at Physics International Company since they have employed a liquid explosive nitromethane in their work.

Several considerations dictated against use of the liquid explosive in the present effort.

These were:

(1) The detonation velocity of nitromethane is sufficiently low as to significantly reduce pressures obtainable in the gas reservoir. To make up for this, requires a much larger device if a high projectile velocity is to be achieved with a steel projectile of $L/D = 6$.

(2) Use of nitromethane can result in detonation due to gas shock pressurization of gas bubbles in the liquid.^{9,10} This results in early detonation and thus pinch off of the pressure tube. To avoid this problem, the Physics International Company currently uses transparent plastic tubes as tamper (container) tubes to make examination for entrapped gas easier.

(3) Solid explosives offer much versatility not available where designs are based on liquid explosives. The use of solid explosive does not require the use of an outside (tamper) tube, and where a tamper is used, it can be made of any convenient material. Solid explosives can be pressed, cast, machined, or cut from Deta Sheet and their use offers a wide variety of explosive material properties from which to choose.

⁹F. P. Bowden and A. Yoffe, Fast Reactions In Solids, Butterworths London, 1958.

¹⁰F. P. Bowden and A. Yoffe, Initiation and Growth of Explosion in Liquids and Solids, Cambridge Press, Cambridge Eng., 1952.

This third reason was not of such immediate consideration, but since the use of a liquid explosive could lead to as many special problems as the use of a solid explosive, it was decided efforts to resolve such problems should be directed toward that avenue that would offer flexibility at BRL in the event further use of explosive drivers were to be undertaken. Among possible future applications might be use of the explosive driver in weapons systems design. Work in this direction has already been undertaken at Rock Island.¹¹

It should be noted also that the primary reason for the choice by Physics International Company for the use of nitromethane was the convenience it offered for the large scale tests they have undertaken. Since large scale tests are not envisioned as a possible outgrowth of the present program, this consideration for use of a liquid explosive was not deemed to be relevant to the BRL needs.

The above considerations resulted in the choice of a solid (cast) explosive, specifically 75/25 octol ($D = 8.48$ km/sec). A practical limit on the length of the explosive driver is set at $L = 1.8288$ m (6 feet). From Equation (10), (17) and (20) we obtain the values for the lengths of the sections of the pressure tube in terms of the pressure tube diameter, d_0 .

Given the pressure tube length, the tube diameter is computed based on the total mass G of light gas required to launch the projectile to a specified velocity and in terms of the loading density ρ_1 for the gas according to

$$G = \frac{1}{4}\pi \rho_1 d_0^2 L \quad (24)$$

The loading density of the pressure tube gas, ρ_1 , is constrained to a somewhat narrow range of values determined by the requirement that jetting of the pressure tube not occur during collapse, and that full collapse of the pressure tube be achievable, as discussed below.

IV. RELATION BETWEEN GAS RESERVOIR AND LAUNCH VELOCITY

Given the mass G of gas at a pressure p_4 in a reservoir of diameter d_0 , ratio of specific heats γ , and sound velocity a_4 for the reservoir gas, a projectile of mass M , traveling a distance x_p in a smooth gun tube of cross sectional area A (diameter d_1) under the pressure exerted by the reservoir gas, will achieve a muzzle velocity u_p given by the Seigel⁷ graphs for gun performance. Figure 6 gives

¹¹J. R. DeWitt, "Weaponization of Increased Speed Projectile: Compendium, 4th General Review," ARO, Inc. February 1975.

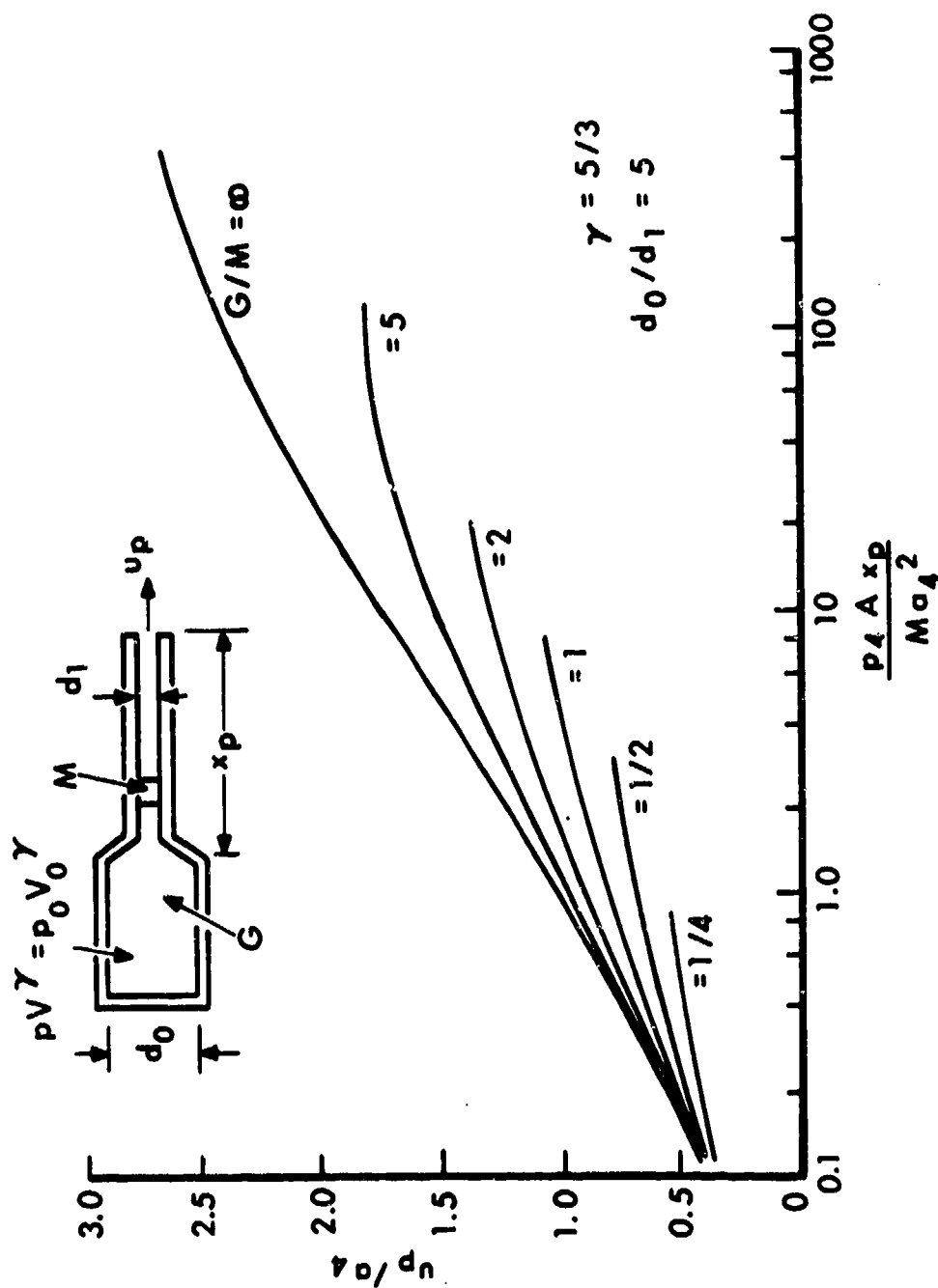


Figure 6 - Design performance curves for reservoir gun, after Seigel⁷, $\gamma = 5/3$, $d_0/d_1 = 5$.

an example of these curves for the nondimensional velocity (u_p/a_4) as a function of the nondimensional projectile travel ($p_4 A x_p / M a_4^2$) at various values of G/M for a light gas with $\gamma = 5/3$ (i.e. as appropriate for helium) and a pressure tube diameter to launch tube diameter ratio of 5 (dependence of the curves on the d_o/d_l ratio is weak) as taken from Seigel.⁷

Given the projectile mass, bore diameter, barrel length, chamber diameter, and desired muzzle velocity, one can compute the required chamber pressure at launch, and the mass of gas required to achieve that velocity. The loading gas pressure and detonation velocity largely determine the final chamber pressure and density. One uses the approximate chamber diameter to bore diameter to obtain the required pressure and density in the pressure tube, leaving only simple calculations to be carried out to determine the actual chamber diameter and overall dimensions of the explosive driver for the final design.

V. LOADING PRESSURE IN THE GAS PRESSURE TUBE

Physics International Company experience with the design of explosive drivers has shown that the gas tube loading pressure must be kept within certain bounds in order to prevent (1) metal jetting (i.e. shaped charge jetting) in the case of a loading pressure that is too low, and (2) failure to fully collapse the pressure tube because the loading pressure is too high. Each of these limits can be calculated if necessary, however, it is simpler to use a pressure that has proved satisfactory in the past. Physics International has employed loading pressures from 1.034×10^5 pascals to 1.690×10^7 pascals. With nitromethane the usual practice has been to use 1.931×10^6 pascals.

Since the explosive used in the present experiment, 75/25 Octol, has a higher detonation pressure than that of the nitromethane used at Physics International, calculations have been made using the detonation pressure scaled value of 2.60×10^6 pascals (377psi) for the pressure tube loading pressure. A higher pressure of 3.45×10^6 pascals (500 psi) has also been used for calculations. This value is somewhat closer to the maximum pressure according to advice obtained from Physics International personnel, but permits a larger value of G as important in the present task.

The outside dimension of the pressure tube in Physics International practice has been about 5% over the inside diameter of the tube where fabricated of steel and operated at a lower pressure, such as the 1.931×10^6 pascals (280 psi) figure mentioned above. The value is not critical, however, and the large Alpha I device tested at Physics International employed a figure of 9.5% at a pressure of 6.448×10^6 pascals (935 psi). At 2.552×10^6 pascals (370 psi), allowing for the difference in density between aluminum (see section VII for the choice of aluminum over steel for the pressure tube) and steel we obtain a value of 2.235 cm (0.88"), and at 3.448×10^6 pascals (500 psi), 3.023 cm (1.19"). Note the wall thickness is not selected on the basis of strength to hold the pressure - The above criterion being in excess of that requirement - but to provide "piston" mass for the compression of the helium to achieve full collapse. If too much mass is used, the device will require too much explosive, becoming excessively inefficient; too little and the momentum of the pressure tube wall will not be sufficient to collapse onto its axis under the high pressure of the helium behind the shock front. In the present design the OD has been taken to 2.54 cm (1.00") greater than ID; for a wall thickness of 1.27 cm (0.5") in the 1.27 cm (0.5") caliber design a value of 0.635 cm (0.25") is used as may be noted in Table I.

The amount of explosive used in the design must be sufficient to drive the pressure tube radially onto the axis at such a velocity, so as to collapse the tube. Again, based on the Physics International practice, a range of values from 0.5 to 2 times the pressure tube mass has been used to calculate the required mass of explosive. Private communication with Physics International people suggested the present device should employ the higher figure even though Octol is more energetic than the nitromethane (the reason being primarily that only a light tamper would be employed, but also the failure to collapse the pressure tube is a more likely problem than that of jetting). The present calculations are based on the charge to mass (of pressure tube) ratio of 2. It should be noted that one can also readily compute the necessary amount of HE simply by using the Gurney¹² equation for the plate (tube wall) velocity as a function of the

¹²R. W. Gurney, "The Mass Distribution of Fragments from Bombs, Shell and Grenades, "BRL Report 448, U.S. Army Ballistic Research Laboratory, Aberdeen Proving Ground, MD, Feb 44.

charge to mass (areal density of the charge and plate, of course) ratio and requiring this to be equal to the velocity needed to just bring the tube mass to rest working against the gas pressure behind the shock (i.e. p_2), allowing for the areal density of the tube wall to increase with decreasing radius. That is to say v_e as given by¹² (we approximate here using the expression for cylindrical expansion where as collapse equations would be more exact):

$$v_e = k \left[\frac{M'}{C} (1 + \frac{1}{2} C/M') \right]^{-1/2} \quad (25)$$

where M' is the pressure tube mass, C the HE charge mass and k is a coefficient for the HE, must also equal v_e as given by integrating for the decelerating tube mass:

$$v_e = (P_2 r_0 / T_p \rho_p)^{1/2} \quad (26)$$

where ρ_p is the density, T_p the thickness, and r_0 the initial inside radius of the pressure tube.

Tamper wall thickness selection is not critical in the present design. Values noted in Table III have been based on machining convenience. The charge to mass ratio selected allows one to use a minimal tamper.

VI. COMPUTED DESIGN: 1/2" CALIBER, 1/4" CALIBER AS TESTED

Table I & III employ the above criteria in the calculation of the critical parameters for the design of explosive drivers having a 1/2" (12.7 mm) diameter launch tube, 1/4" (6.35 mm) diameter launch tube, and 0.281" (7.14 mm) diameter launch tube as fabricated. Projectile mass and launch velocity are determined by the application of the explosive driver gun in the test of an explosive muzzle accelerator device¹³. The explosive is selected for its high detonation velocity and convenience as a castable material. Table II shows the considerations leading to a selection of $G/M \approx 2$. A value of $G/M \approx 2$ is required to achieve a projectile velocity u_p of at least 6 km/sec.

¹³ H. Walker, "Acceleration of Hypervelocity Projectiles by Means of Transversely Expanding Gas," (in preparation).

TABLE I. Computed and As Tested Driver Design

	1.27 cm (1/2") design	0.635 cm (1/4") design	As Tested
Caliber d_1	1.27 cm	0.635 cm	0.714 cm
Projectile Mass M	36.49 g	4.56 g	6.36 g
Press. Tube Dia. d_0	11.43 cm	5.715 cm	5.715 cm
He load Press. P_1	2.55×10^6 Pa	2.55×10^6 Pa	3.45×10^6 Pa
Gas Density ρ_1	4.23×10^{-3} g/cm ³	4.23×10^{-3} g/cm ³	5.71×10^{-3} g/cm ³
Explosive	75/25 Octol	75/25 Octol	75/25 Octol
Detonation Vel. D	8.48 km/s	8.48 km/s	8.48 km/s
Shocked Sound Vel. a_2	9.75 km/s	9.75 km/s	9.75 km/s
Reservoir Press. P_4	2.43×10^9 Pa	2.43×10^9 Pa	3.29×10^9 Pa
Reservoir Density ρ_4	4.23×10^{-2} g/cm ³	4.23×10^{-2} g/cm ³	5.71×10^{-2} g/cm ³
Barrel Length x	3.658 m	1.829 m	1.918 m
\bar{x}	0.325	0.325	0.417
G/M	2.175	2.175	2.108
Muzzle Vel u_p	6.3 km/s	6.3 km/s	~ 6.3 km/s
G	79.4 g	9.93 g	13.4 g
Press. Tube Dia. d_0	11.43 cm	5.715 cm	5.715 cm

TABLE I. Computed and As Tested Driver Design (cont.)

	<u>1.27 cm (1/2") design</u>	<u>0.635 cm (1/4") design</u>	<u>As Tested</u>
Press. Tube Length L	1.83 m	0.91 m	0.71 m
Reservoir Length L _R	13.72 cm	6.86 cm	6.86 cm
Press. Tube Thick. T _p	1.27 cm	0.635 cm	0.635 cm
HE ID	13.97 cm	6.99 cm	6.99 cm
HE OD	19.69 cm	9.84 cm	9.84 cm
Mass of HE C	56 kg	7 kg	8.7 kg
HE to Press Tube: C/M'	2.01	2.01	2.01
Tamper Wall Thick.	0.953 cm	0.476 cm	0.476 cm

TABLE II. Values of u_p , projectile muzzle velocity, for choices of G/M_p , ratio of gas (reservoir) to projectile mass, for $\bar{x} = 0.325$ and $d_0/d_1 = 5$. The requirement to achieve $u_p \geq 6.0$ km/sec is indicated by asterisk. (The corresponding L and d_0 dimensions are given below.)

G/M	u_p
1/2	5.46
1	5
2*	6.24*
5	6.44

* $G/M = 2$, $L = 1.829$ m (6 ft.) requires $d_0 = 10.96$ cm (4.315") (1/2" design)

TABLE III. Computed and Fabricated Design Parameters

	<u>1.27 cm (1/2") design</u>	<u>0.635 cm (1/4") design</u>	<u>Design as Fabricated & Tested</u>
G/M	2.175	2.175	2.108
u_p (Projectile muzzle velocity)	6.3 km/s	6.3 km/s	6.3 km/s
G	79.40 g	9.925 g	1341 g
d_0	11.43 cm (4.5")	5.715 cm (2.25")	5.715 cm (2.25")
L	1.8288 m (6')	0.9144 m (3')	0.9144 m (3')
L_g	1.234 m (48.6")	0.617 m (24.3")	0.617 m (24.3")
L_R	13.72 cm (5.4")	6.86 cm (2.7")	6.86 cm (2.7")
Press. Tube Thickness T_p	1.27 cm (0.5")	0.635 cm (0.25")	0.635 cm (0.25")
HE ID	13.97 cm (5.5")	6.985 cm (2.75")	6.985 cm (2.75")
HE OD	19.685 cm (7.75")	9.843 cm (3.875")	9.843 cm (3.875")
C (Mass of HE)	56 kg	~7 kg	7 kg
Tamper Wall Thickness	0.953 cm (3/8")	0.476 cm (3/16")	0.476 cm (3/16")
C/M	2.01	2.01	2.01

The design as fabricated is shown in Figure 7 together with the design of the projectile and sabot used. The chamber block dimensions have been scaled from the dimensions as used in Physics International practice and modified slightly after discussions with Physics International personnel. Specifically, the ratio of outer diameter (20.32 cm (8")) in the device as fabricated to inner diameter of the chamber (5.715 cm (2.25")), 3.56, is about the same as employed in the Alpha I design ($56'' / 16'' = 3.50$).

The reservoir length to diameter ratio (16 in the present design) is smaller than in the Physics International practice (where a value of 30 is used) as a result of the decision to make HE casting more manageable. The breech bevel ring section of the chamber block (designed to close the gas reservoir) was originally also scaled down proportionately. Discussions with Physics International personnel indicated that this section should not be reduced in length. As a result, the breech bevel ring as shown in Figure 7 is long as compared to the length of the reservoir, but is in proportion (after Physics International practice) to the reservoir diameter.

VII. HIGH EXPLOSIVE INDUCED BARREL CLOSURE

In the Physics International practice using small L/D, low density projectiles, projectile acceleration was sufficiently high to avoid damage to the projectile caused by constricting the barrel of the gun onto or ahead of the projectile (shocks in the driver gas has caused damage to the projectile in the Physics International experiments, but this problem has been solved by placing the projectile $\frac{1}{4}$ caliber into the bore). In the Physics International tests the projectile moved sufficiently rapidly down the barrel to remain ahead of these shocks. With high L/D, high density projectiles this problem is much more severe. Calculation indicated however, that this problem could be overcome if the base pressure were chosen to be high. Figure 8 shows a plot of the earliest arrival time for shocks generated by the HE traveling through the chamber block illustrated in Figure 7 as a function of position down the barrel using the base pressures as given in Table I. The abscissa in Figure 8 represents the barrel position with $x = 0$ located at the entrance to the bore at the front face of the chamber. The plot extends to 8.890 cm (3.5 inches), which corresponds to the front face of the chamber block. Also, shown in Figure 8 are curves representing the projectile position, one for the rear most point on the steel projectile (the base cone apex) and one for the position of the bourrelet as a function of time based on the assumption of uniform acceleration at the computed pressure as given in Table I for the design as fabricated and tested. It will be seen that the device as designed just satisfies the requirement that the projectile clear the chamber block before the earliest detonation shock arrives at the projectile.

Consideration has also been given to the problem of complete closure of the bore due to HE shocks propagating through the chamber block. Elementary calculations taking into consideration only the inertia of the chamber block and the approximate velocity imparted to the chamber block based on charge (on the breech section) to mass (of the entire chamber block) ratio (ignoring strength affects) indicate that constriction should not occur before the projectile exits the barrel. Taking into account the strength of the steel, again in an approximate calculation, indicates the shock should not be sufficiently large to collapse the bore. A proper resolution of this point requires hydrocode modeling. The problem was put on the computer using the HELF code. Unfortunately, the time steps became prohibitively small at the corners of the block preventing completion of the analysis (with the available personnel time for modification of the problem to resolve the divergencies encountered in the tasks).

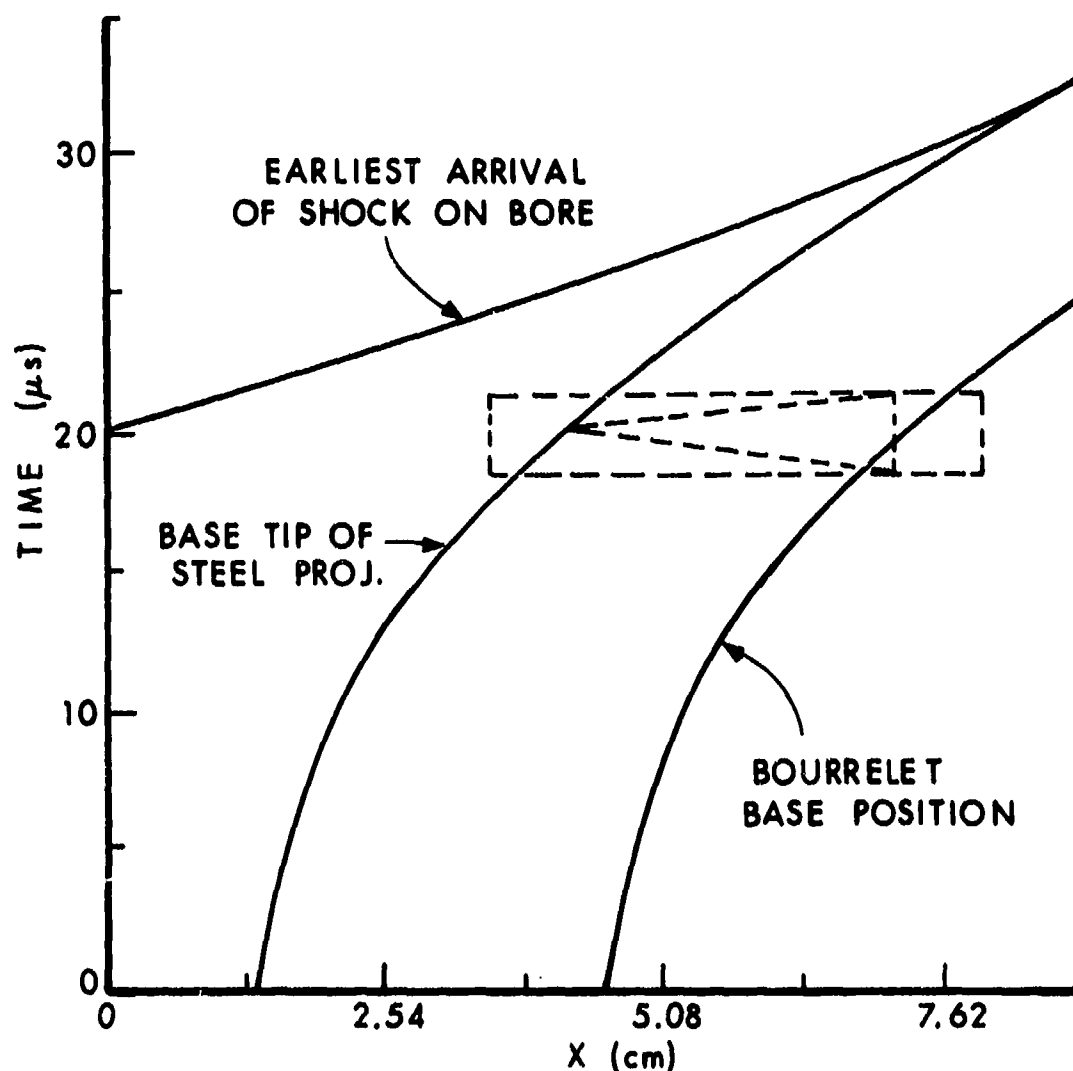


Figure 8 - Plot of calculated earliest time of arrival for shock as a function of bore position, together with position of projectile as function of time under uniform acceleration. Time $t = 0$ corresponds to the arrival time of the gas shock at the bore entrance, $x = 0$. Maximum value of x corresponds to the front face of the chamber block. Two projectile curves are shown together with a schematic of the projectile to indicate the feature corresponding to each curve.

VIII. SELECTION OF MATERIALS

The chamber blocks material employed in the present experiment is annealed 4340 steel, a tough steel having a high value for the maximum elongation (to allow breech closure without brittle failure). The question of the failure of the breech on closure is a difficult question that must be answered by experiment.

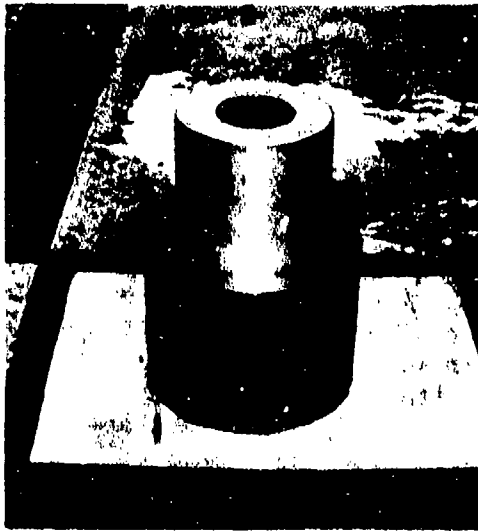
Figure 9a shows a chamber block fabricated to test for closure, with the same dimensions as shown in Figure 7. An aluminum collar 12.70 cm (5") inside diameter and 12.70 cm (5") in length was used to cast the ring of Octol around the breech bevel ring of the chamber block. Detonation was achieved using a circular section of Deta sheet placed on top of the cast Octol together with a detonator and booster placed at the center of the Deta sheet. Figure 9b shows a tracing taken from the resulting flash x-ray at 800 μ s after detonation indicating that the bevel ring has collapsed and rebounded. The required confinement is 1 ms so the total HE around the bevel ring has been reduced to that indicated in Figure 7. The test shown in Figure 9 did not involve any pressure tube gas. The presence of such gas will decelerate the bevel ring during collapse reducing the impact forces responsible for the recoil observed in Figure 9.

The pressure tube itself poses a severe problem. It is to be remembered that the Physics International Company customarily employed very low density projectiles, such as Lexan or the lithium - magnesium alloy LA141A having a density of 1.38 g/cm³, and L/D values as low as 0.8; a value of L/D = 1.64 g/cm³ was employed for a lithium - magnesium alloy projectile in the Alpha I test. In the present experiment the projectile has an L/D = 5.3 and a density of 8.0 g/cm³. This means that the time required for the projectile to exit the barrel is much greater proportionately (by a factor of 18.7) than for the Physics International Company test of the Alpha I design. This means that in addition to the problems of gas confinement without chamber rupture, there is the problem that heat loss from the driver gas to the chamber wall must be kept to a minimum.

The temperature of the helium gas in the reservoir for the device as tested (i.e. column 3, Tables I & III) is computed to be

$$T_4 = T_1 p_4 \rho_1 / p_1 \rho_4 = 28620^\circ\text{K} \quad (27)$$

for an initial gas temperature of 300°K. For a launch time of $\Delta t \approx 1$ ms, black body thermal radiation to the walls will involve a total energy of



(a)

(b)

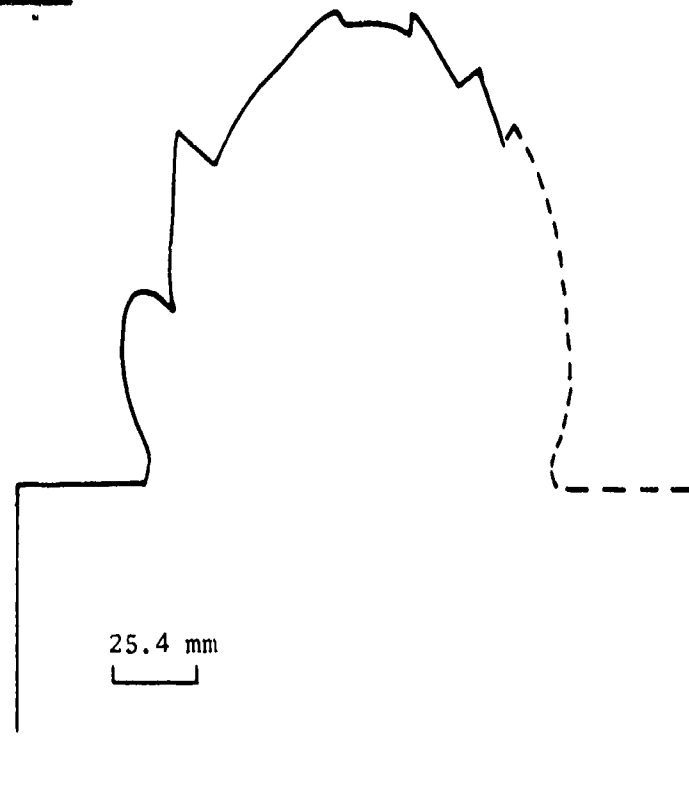


Figure 9 - Photograph of the test chamber block used to determine adequacy of the breech bevel ring dimensions. The top figure (a) shows the chamber block with an aluminum collar placed around the bevel ring. Octol has been cast in the space between the aluminum collar and the bevel ring. The bottom figure (b) shows a tracing taken from the flash x-ray 800 μ s after detonation of the Octol.

$$E = \sigma T^4 A_{\text{Res}} \Delta t = 0.629 \text{ MJ} \quad (28)$$

The PV energy of the gas, however, is only 0.536 MJ. One also finds that the optical thickness of the helium gas at a density of $5.7 \times 10^{-2} \text{ g/cm}^3$ is quite large for 3 ev photons. Thus, it is clear that unless the walls of the pressure tube are highly reflective, 90% reflective or better, a substantial degradation in projectile launch velocity must be expected. Essentially all materials that might be employed for the pressure tube fail to meet this requirement.^{14,15} Steel readily absorbs 3 ev photons.

Aluminum is a singular exception^{14,15} as may be seen from the data in Figures 10 and 11. The reflectance is 90% and better in the photon energy range of interest except for a narrow absorption peak at 1.5 ev. for which reflectance is only about 75%.

The high reflectivity characteristic of aluminum has been incorporated into the explosive driver design. As will be noticed in Figure 7, not only is the pressure tube aluminum, but an aluminum face plate is located at the front of the reservoir to reduce radiation loss. Radiation loss to the gun bore wall remains a problem, however. Aluminum plating of the gun barrel bore has not been undertaken in the present test, but should be a prime consideration in any future tests.

It may be mentioned that failure to employ aluminum as a reservoir and bore wall liner material may have been the cause of the failure to achieve high velocities in several explosive driver tests at Physics International and elsewhere, and may be a serious short coming facing the two stage explosive driver performance mentioned above.⁵

¹⁴F. Abelès, "Optical Properties of Metals," in Optical Properties of Solids edited by F. Abeles, North-Holland Publishing Co., Amsterdam, 1972.

¹⁵H. Ehrenreich, "Electromagnetic Transport in Solids: "Optical Properties and Plasma Effects," in Rendiconti della Scuola Internazionale di Fisica "Enrico Fermi" XXXIV Corso: Proprietà Ottiche Dei Solidi, edited by J. Tauc, Academic Press, New York, 1966.

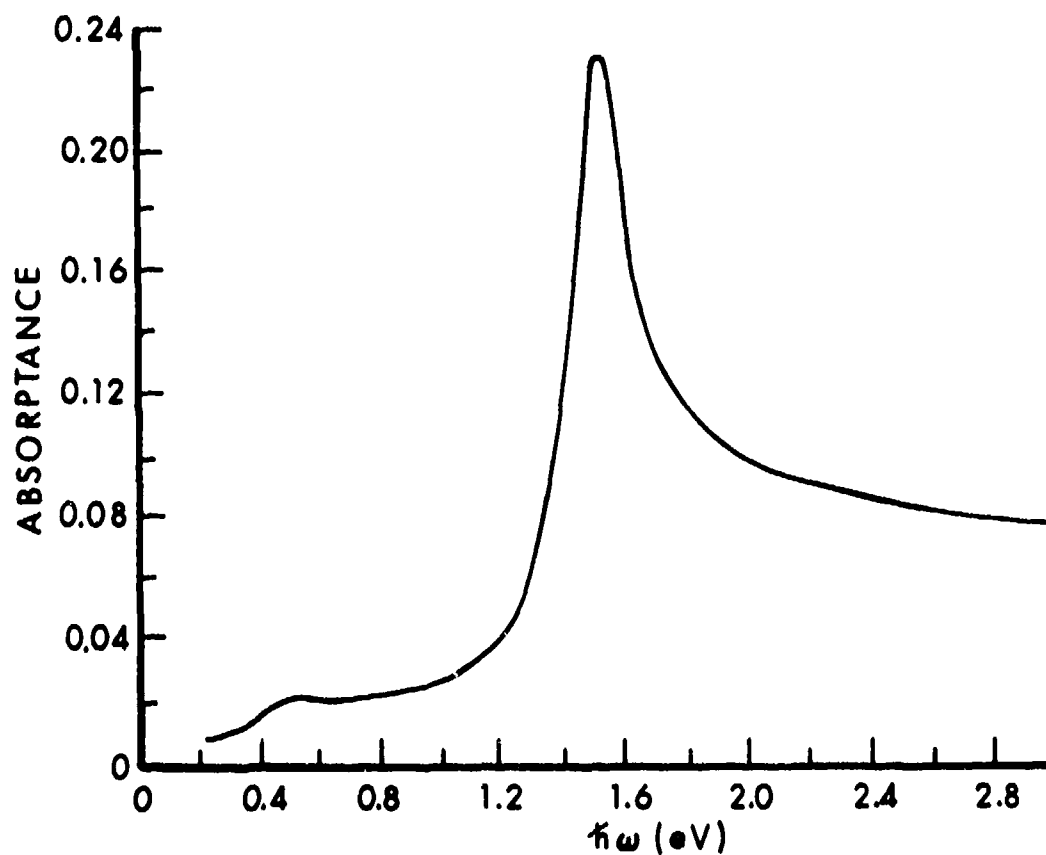


Figure 10 - Absorptance (ratio of absorbed to incident energies) for pure aluminum ¹⁴ as function of photon energy.

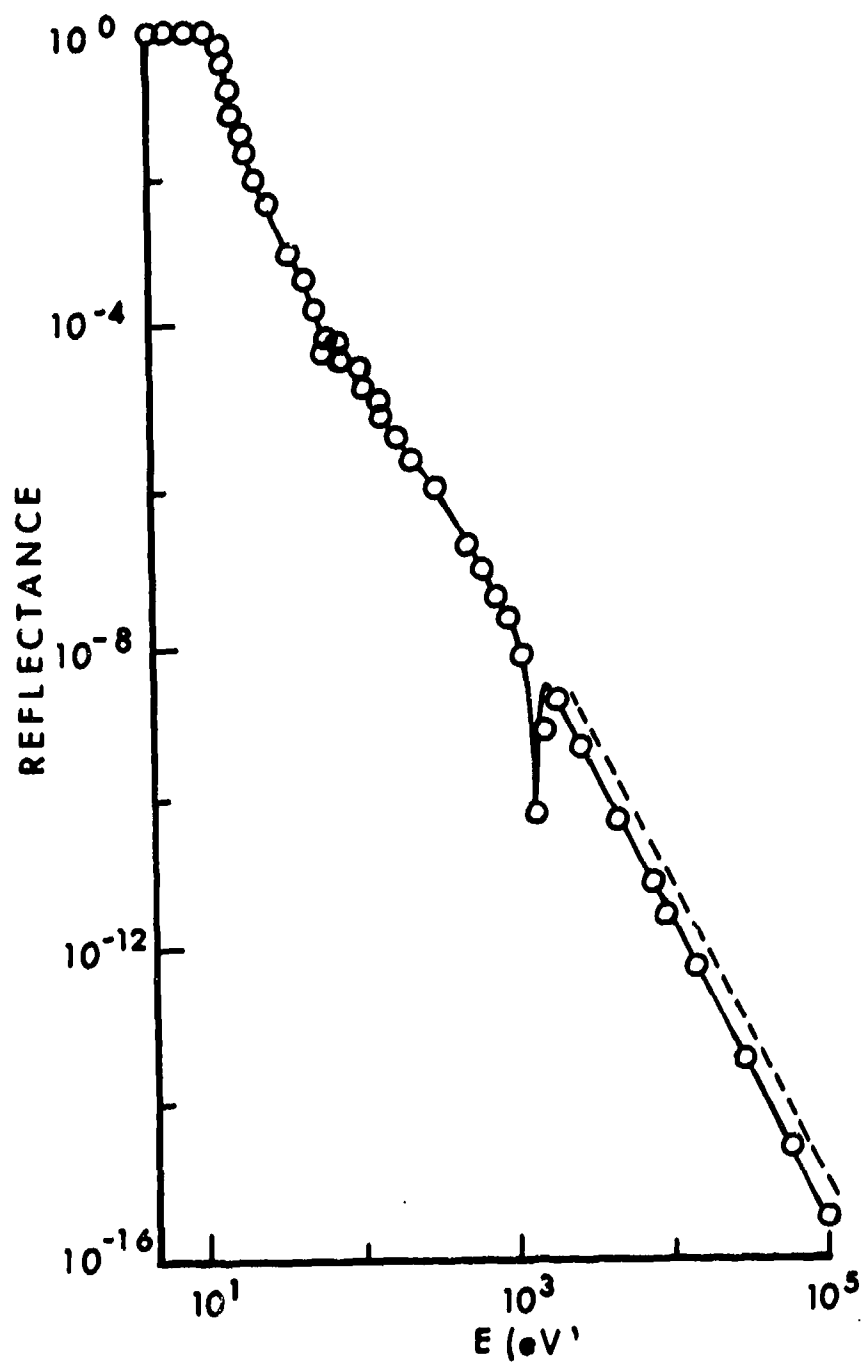


Figure 11 - Reflectance of photons for aluminum ¹⁵ as function of energy.

IX. TEST SET UP, PROCEDURE AND DIAGNOSTICS

The experimental set up employed the explosive driver for the 0.281 inches (0.714 cm) bore barrel as detailed under the "as tested" columns in Tables I and III. Explosive, 75/25 Octol, was cast and cut flush to the end of the tamper. A cylindrical cavity in the high explosive was formed extending from the end of the pressure tube to the end of the tamper by setting a 2.75 inch (6.79 cm) diameter riser over the end of the pressure tube and casting around it. This cavity allowed any helium gas leaking from the pressure tube to vent rather than build up pressure on the explosive. A 1/2 inch (12.7 mm) disc 4 inches (10.16 cm) in diameter with a booster cavity at the center and a 3/4 inch (1.91 cm) diameter off center hole for the vacuum/helium pressure line to pass through was taped to the end of the explosive driver to provide uniform detonation of the explosive in the driver. The projectile was placed in its polycarbonate sabot and epoxied one caliber into the bore in the chamber block.

The barrel was screwed into the chamber block and tightened. Measurements were taken to assure complete seating of the barrel in the chamber block and epoxy (fast setting) was used on the threads to help seal the barrel so that a vacuum could be drawn on the bore.

A special fixture as shown in Figure 12 was attached to the end of the barrel. This fixture served to provide the following functions:

- (1) seal the barrel with a thin steel cap that the projectile could penetrate
- (2) provide connections to evacuate the barrel
- (3) house a thin walled tube of Baratol (part of a separate test program)
- (4) provide x-ray windows in the support structure for the Baratol tube (slots machined into support tube).
- (5) provide break wire to fire second x-ray during passage of projectile through the Baratol
- (6) provide a barrel section having two spaced 0.025 mm diameter break wires to measure velocity before entering the baratol tube and to fire first x-ray tube and an x-ray window (groove machined into barrel section).
- (7) provide a free flight section with two spaced 0.076 mm diameter break wires to trip counters (for time measurement to obtain velocity measurement after passage through the baratol tube) and fire third flash x-ray.

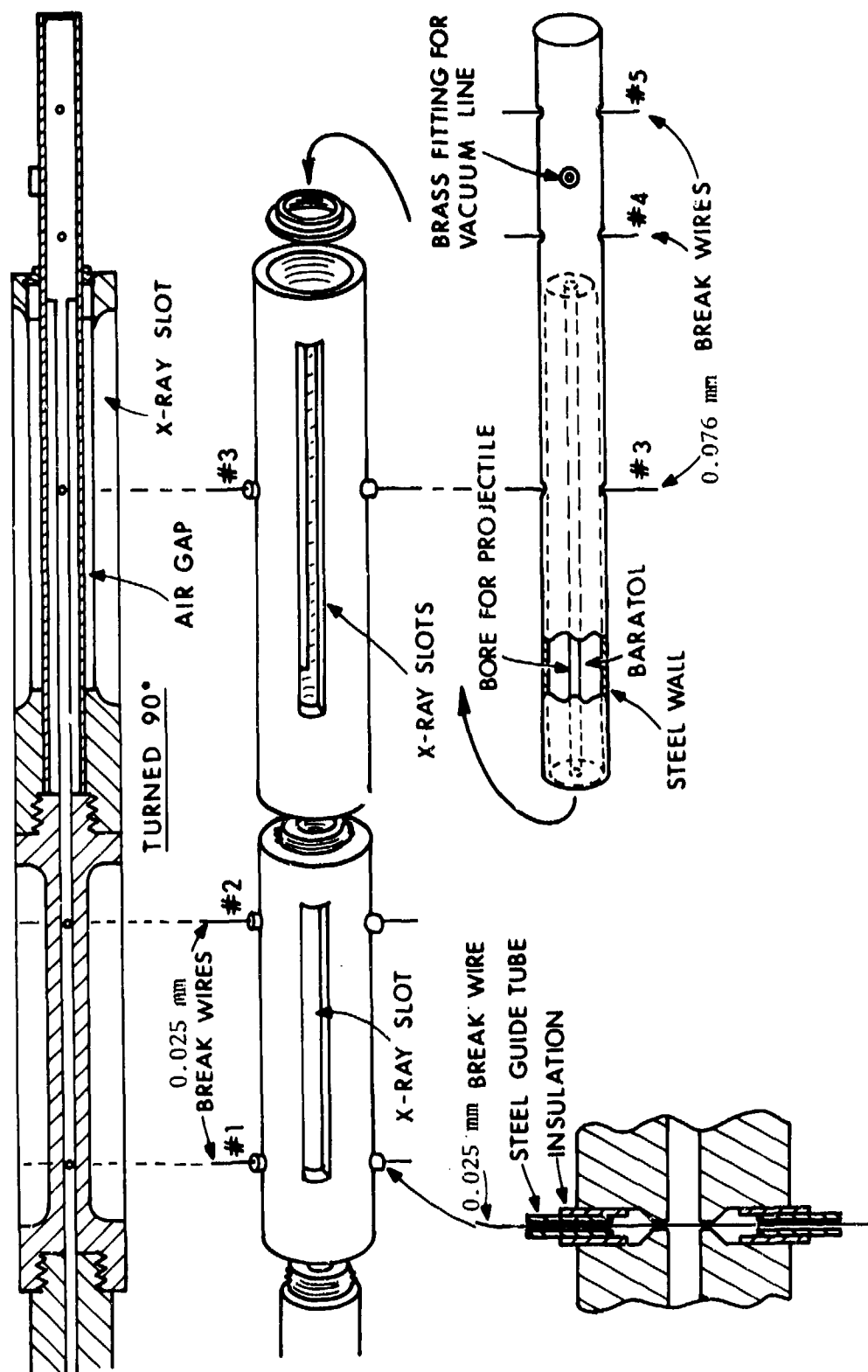


Figure 12 - Fixture to hold baratol tube, vacuum line hookup, break wires, x-ray "windows," and projectile exit "window," as tested.

The complete assembly was set up on a 3.66 m long table designed to cradle the explosive driver gun with its attachments and to support the gun in from of the flash x-ray tubes. The set up is shown in Figures 13, 14 and 15. The three ports for the flash x-ray tubes can be seen in Figures 13 and 15 (The photographic film holders are not shown in these figures). Figure 13 shows the entire device, with the explosive driver on the right, the 1.83 m long barrel in the center and at the left, the explosive tube holder, break wire connections and free flight section. Figure 14 shows the chamber block to the left, tamper containing the cast explosive and pressure tube, and to the right the explosive disk taped to the tamper with the copper tubing vacuum/helium gas line extending out to the right.

Figure 15 shows the end of the gun barrel at the right connected to a slotted aluminum barrel extension containing two 0.025 mm diameter break wires. Connectors for these wires can be seen extending above and below this aluminum section at each end of the slot.

The 0.025 mm break wires were inserted into the 1.6 mm narrowing to 0.8 mm holes using a hypodermic needle as a guide. One inch sections of the hypodermic needle soldered to the break wires were used as electrical connection posts. These posts were insulated from the barrel with sections of wire insulation and epoxyed to the barrel to provide support and vacuum seals. The break wires were tested to make sure they could carry sufficient current to trip the timing circuits and fire the flash x-ray units and to check that they were properly insulated from the barrel.

To the left of Figure 15 is a free flight tube also containing a break wire (0.076 mm diameter) to each end. A copper vacuum line can be seen attached to the bottom of this third section of the barrel attachment fixture. In the background lie the three ports for the flash x-ray tubes. Alignment between the three sections of the attachment fixture and the three x-ray ports was adjusted, and protective covers placed over these ports subsequent to taking this photograph. A "static" flash x-ray was taken to check for x-ray penetration of the tubes in this position which proved to be satisfactory.

Figure 16 gives a view looking down the length of the device from the explosive driver end with a 10.16 cm armor steel block in place as target. Yellow paint has been placed on the target block for identification (the test area has several such blocks in the vicinity.)

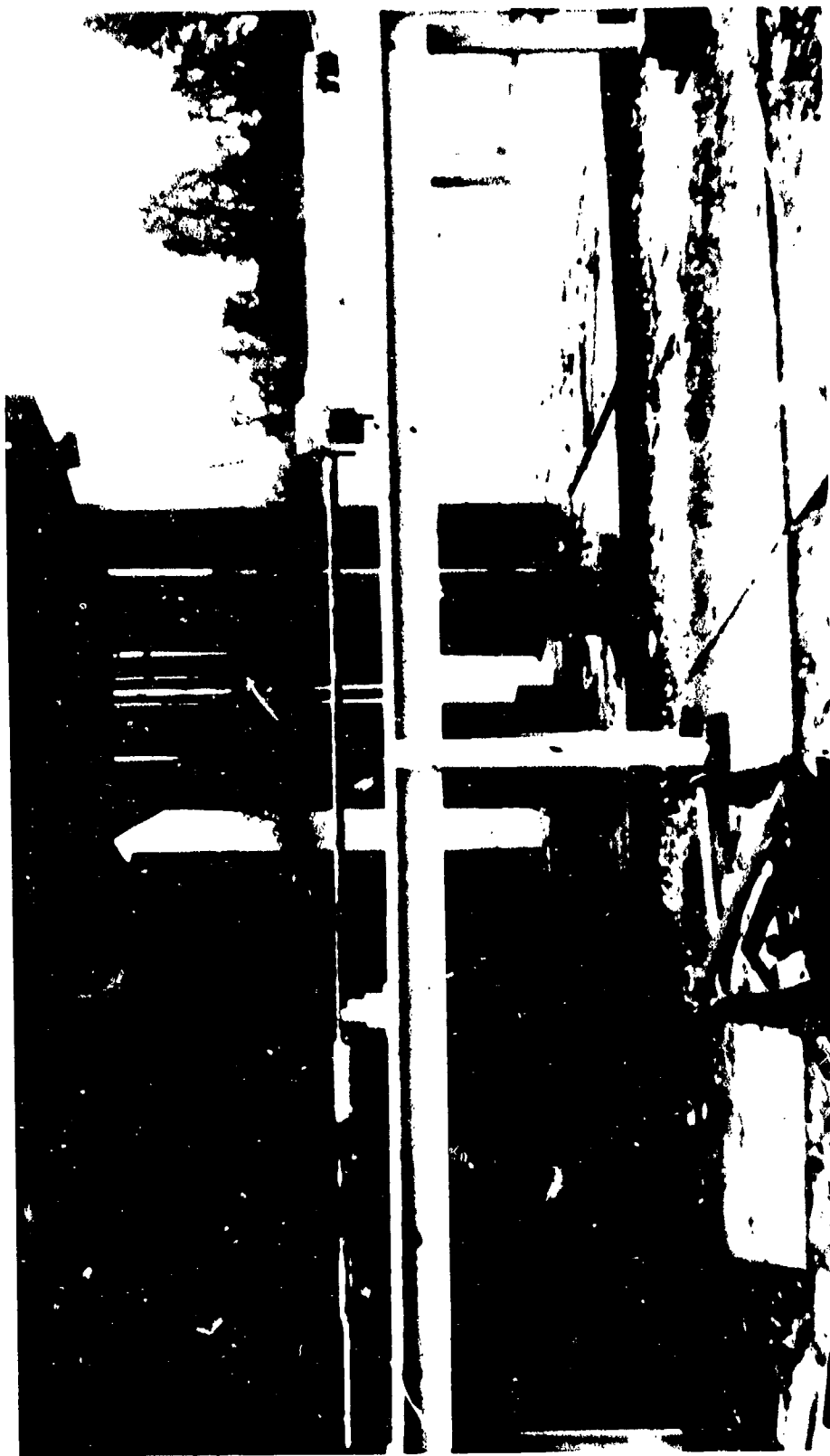


Figure 13 - Photograph of explosive driver gun as tested. The device is mounted on a table with the explosive driver on the right, the gun barrel in the center and the muzzle accelerator device (shown schematically in Fig. 12) to the left. Behind the muzzle accelerator are the three x-ray ports.

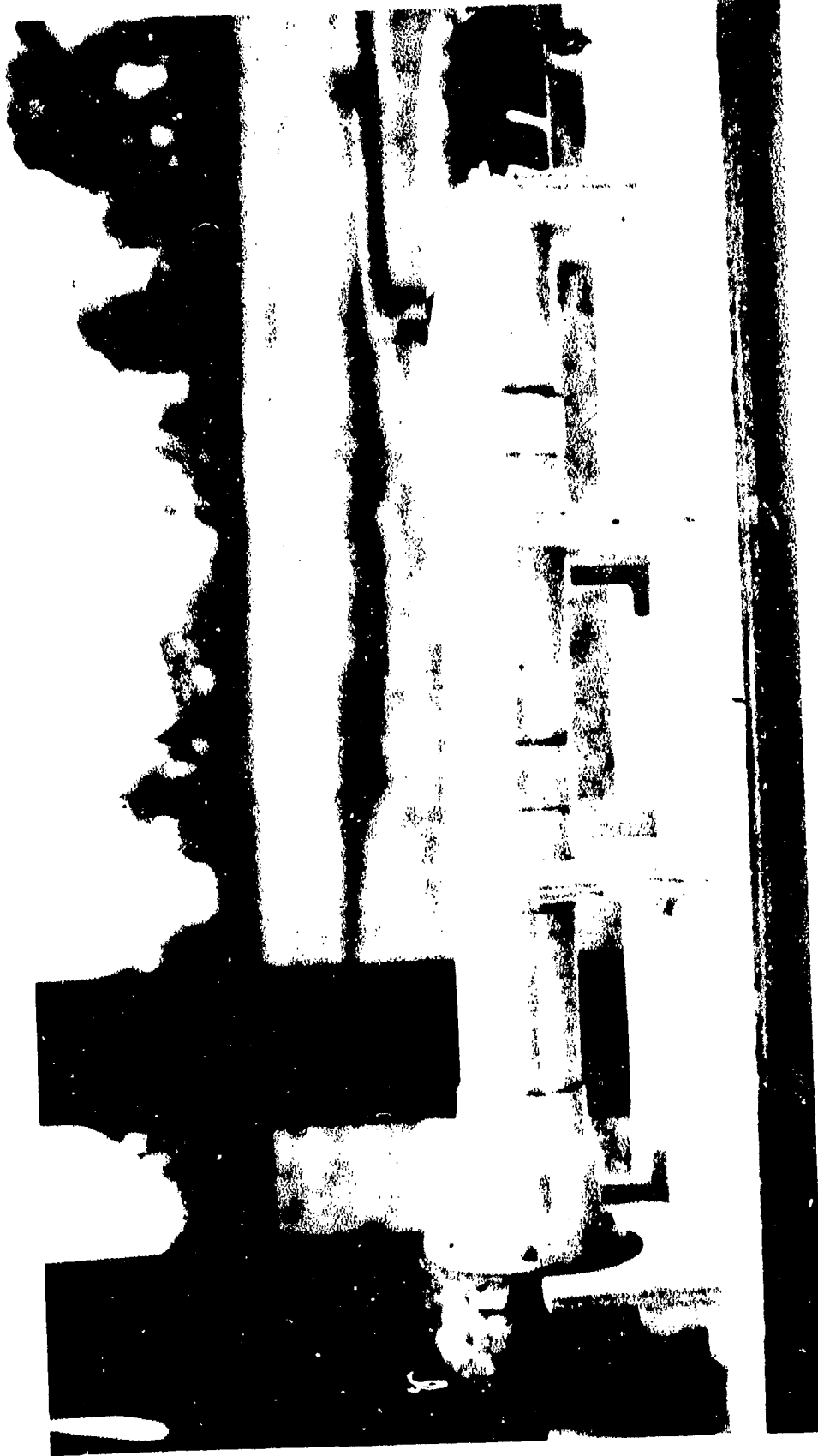


Figure 14 - Photograph of the explosive driver. The chamber block lies to the left. The aluminum tamper containing the cast explosive and pressure tube is in the center. The explosive disk taped to the tamper is at the far right of the photograph.

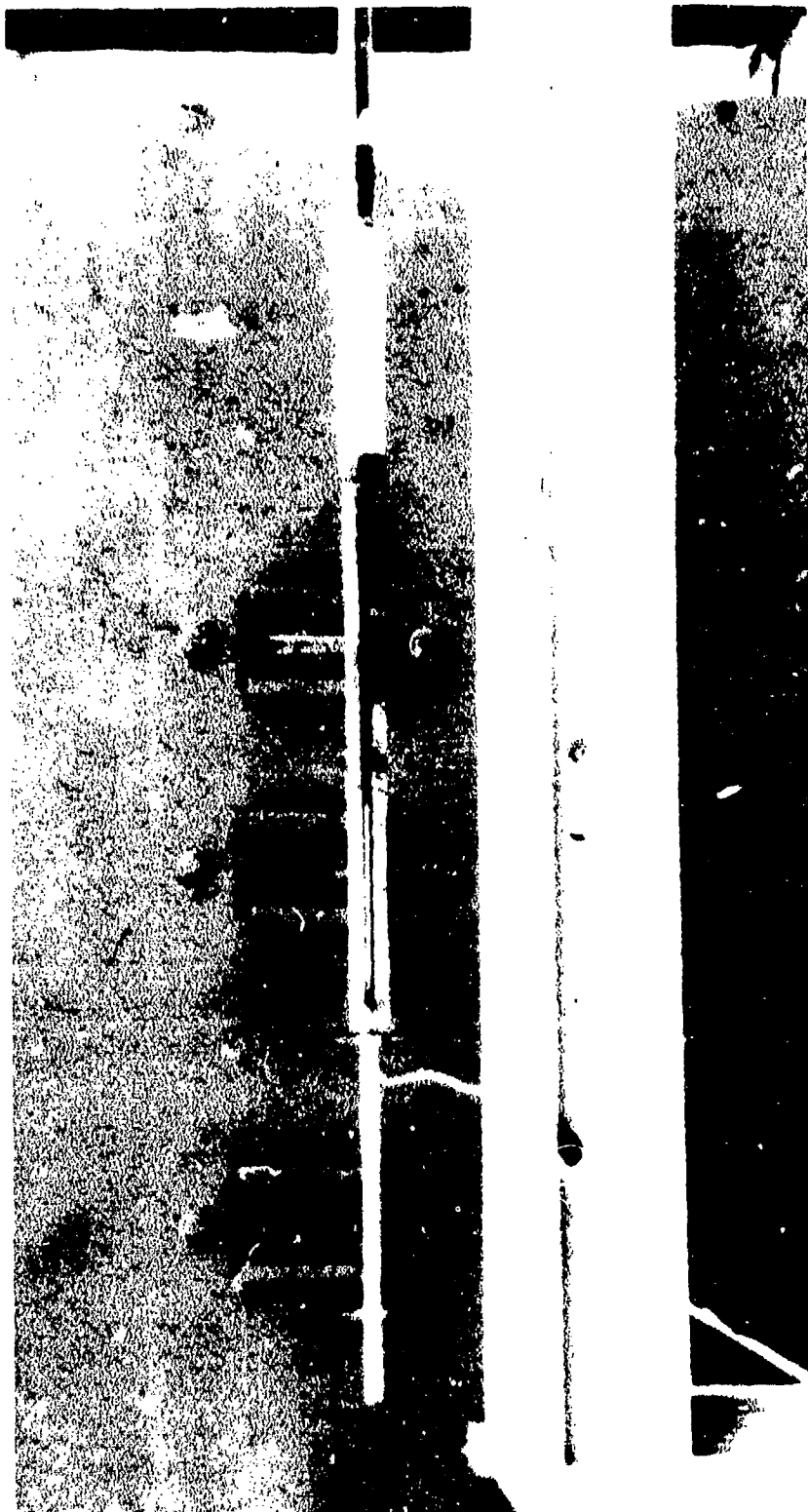


Figure 15 - Photograph of the muzzle accelerator device and velocity "screens" (break wire fixtures). At far right is the end of the barrel of the explosive driver gun. Attached to this is a section of aluminum containing two break wires in a free run section of tube to permit muzzle velocity determination. The tube has been slotted to permit flash x-ray photography of the projectile. The narrow tube at far left is also a free run tube section for velocity determination on exit from the muzzle accelerator device lying between these two sections. A gas line used to pump down the bore is seen on the left. Three x-ray ports can be seen behind the gun.

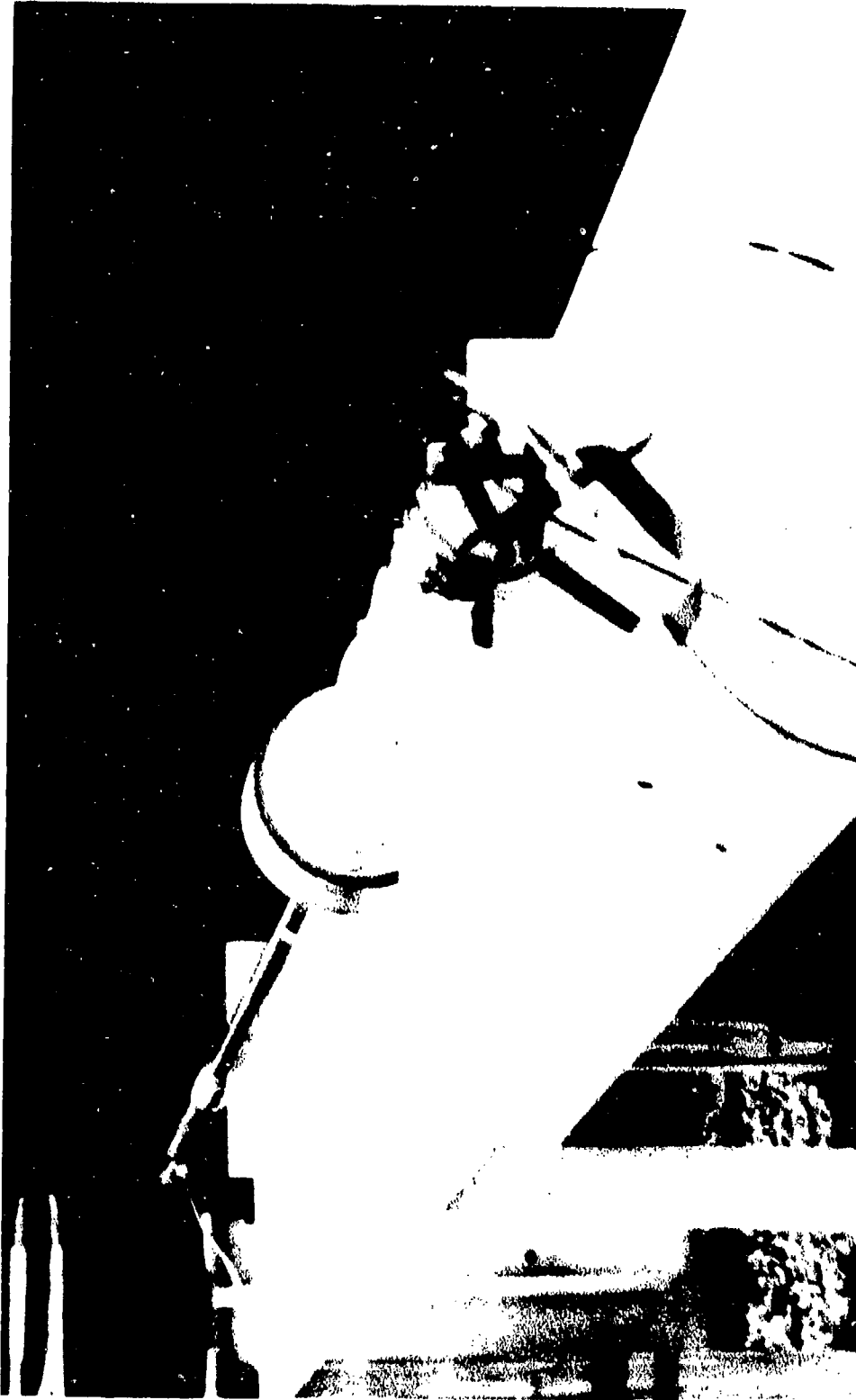


Figure 16 - Photograph of the explosive driver gun looking down the length of the device. In the foreground is the explosive disk used to initiate the driver. One can also see the gas lines used to purge and fill the pressure tube with He. In front of the gun is a 4" armor block target. To the right are the three x-ray ports.

The test procedure included the following steps (list does not itemize safety procedures employed):

- (1) attach and check integrity and functioning of the timing counters on the break wires (manual disconnect of wire)
- (2) check functioning of x-ray tubes to assure breaking circuits would fire x-ray units
- (3) check alignment and measure positions relative to x-ray units
- (4) attach detonator wires
- (5) pump down pressure tube and bore connected by a common line to the oil vacuum pump
- (6) use valves to close off pressure tube from vacuum pump and turn on line connecting pressure tube to 1500 psi helium tank. Maintain bore under vacuum with connection to vacuum pump left open
- (7) pressurize pressure tube to 500 psi (gage)
- (8) fire detonator
- (9) check data on timing counters
- (10) check to ascertain that x-ray units fired
- (11) collect x-ray film cassetts and target block
- (12) collect other items of interest from test site.

X. TEST RESULTS

One device as described above has been tested yielding negative results as to the utility of the explosive driver to launch high density, high L/D projectiles by the present approach. The projectile was not launched down the bore more than approximately 15 cm. The high L/D appears to have caused the projectile to become unstable and to have been driven into the side of the bore.

The calculated velocity between the first and second break wire was 1.86 km/s while a higher velocity of 3.29 km/s was obtained further along the intended path of the projectile between the 4th and 5th break wires. Although the thin rupture disk was broken open, no damage was done to the steel target block. As a result it is clear that the measured velocities resulted from individual (small fragments, shocked gas, or shock traversing the barrel. No fragments were

observed on the flash x-rays although the flash times corresponded to the times of the tripping of the break wires.

The bore of the gun was not closed off by shocks from the HE. The principal malfunction of the device resulted from the shearing of the end of the chamber block about 2 cm around the bore. This sheared steel was shoved down the bore of the barrel, as can be seen in the photograph of the end of the barrel section shown in Figure 17a. Figure 17b shows a side view of the chamber block end of the barrel as recovered.

Unfortunately, neither the pressure tube nor identifiable fragments of the tube were found after the test. The tube would have provided data regarding the adequacy of the driver functioning. The chamber block as expected was broken into numerous parts by the pressure in the reservoir. The recovered parts indicated the chamber block ruptured under tension.

XI. CONCLUSIONS

The primary purpose of the task reported here was to determine the feasibility and utility of explosive driver light gas guns for the launch of high density, high L/D projectiles to hypervelocity. The present design and test study indicate the following :

(1) Use of explosive drivers involves numerous difficulties that are not readily resolved without a specific test program to resolve the difficulties.

(2) While failure to achieve the design velocity for the required projectile does not mean these requirements cannot be met, it does indicate more study and testing would be required to resolve the difficulties.

(3) Although it is well known that launch of projectiles to hypervelocities involves quite large devices, which limits their practicality, for high density, high L/D projectiles the size of the device becomes an especially serious limitation.

(4) Options to resolve the problems encountered impose other limitations and difficulties. Launch instability and shearing of the chamber block into the gun bore can be alleviated by reducing chamber pressure, but this change requires much longer projectile travel, a much larger reservoir, and longer confinement times in the reservoir.

(A)



(B).



Figure 17 - End of barrel attached to chamber block as recovered.
(A) End view showing conical plug of sheared steel from
the chamber block and the enlarged bore. (B) Side view.

(5) In any future tests of the explosive driver gun as designed here, the bore facing the reservoir should be countersunk at a 45° angle and opened to a diameter of about 5 cm. The shape of the pressure tube must be changed to include a mating conical section to fit the countersunk bore. The projectile should have a steel sabot to increase the stability of the projectile in the bore and the projectile should be placed considerably further in the bore initially. Also, the loading pressure in the pressure tube should be reduced by about 1/3 to 1/2.

REFERENCES

1. J.D. Watson, E.T. Moore, Jr., D. Mumma, and J.S. Marshall, "Explosively Driven Light Gas Guns," PIFR-024/065, Physics International Company, San Leandro, CA, Sep 67.
2. E.T. Moore, Jr., "Explosive Hypervelocity Launchers," NASA CR-982, National Aeronautics and Space Administration, Feb 68.
3. J.D. Watson, "An Explosively Driven Gun to Launch Large Models to Re-entry Velocities," PIFR-098, Physics International Company, San Leandro, CA, Apr 69.
4. J.D. Watson, "High Velocity Explosively Driven Guns," PIFR-113, Physics International Company, San Leandro, CA, Jul 69.
5. J.D. Watson, "A Summary of the Development of Large Explosive Guns for Re-entry Simulation," PIFR-155, Physics International Company, San Leandro, CA, Aug 70.
6. E.T. Moore, Jr., "Explosive Hypervelocity Launchers," PIFR-051, Physics International Company, San Leandro, CA, Sep 76.
7. A.E. Seigel, The Theory of High Speed Guns, published by North Atlantic Treaty Organization: AGARD ograph-91. Reproduced by National Technical Information Service, Springfield, VA 22151, May 65.
8. R. Von Mises, Mathematical Theory of Compressible Fluid Flow, Academic Press, 1958.
9. F.P. Bowden and A. Yoffe, Fast Reactions In Solids, Butterworths London, 1958.
10. F.P. Bowden and A. Yoffe, Initiation and Growth of Explosion in Liquids and Solids, Cambridge Press, Cambridge, Eng., 1952.
11. J.R. Dewitt, "Weaponization of Increased Speed Projectile: Compendium, 4th General Review," ARO, Inc., Feb 75.
12. R.W. Gurney, "The Mass Distribution of Fragments From Bombs, Shell, and Grenades," BRL Report 448, US Army Ballistic Research Laboratory, Aberdeen Proving Ground, MD, Feb 44.
13. E.H. Walker, "Acceleration of Hypervelocity Projectiles by Means of Transversely Expanding Gas," (in preparation).
14. F. Abeles, "Optical Properties of Metals," in Optical Properties of Solids edited by F. Abeles, North-Holland Publishing Company, Amsterdam, 1972.
15. H. Ehrenreich, "Electromagnetic Transport in Solids: Optical Properties and Plasma Effects, in Rendiconti della Scuola Internazionale di Fisica, Enrico Fermi" XXXIV Corso: Proprieta Ottiche Dei Solidi, edited by J. Tauc, Academic Press, New York, 1966.

DISTRIBUTION LIST

<u>No. of</u> <u>Copies</u>	<u>Organization</u>	<u>No. of</u> <u>Copies</u>	<u>Organization</u>
12	Commander Defense Technical Info Center ATTN: DDC-DDA Cameron Station Alexandria, VA 22314	1	Commander US Army Communications Rsch and Development Command ATTN: DRDCO-PPA-SA Fort Monmouth, NJ 07703
2	Commander US Army Materiel Development and Readiness Command ATTN: DRCDMD-ST DRCDE-DW 5001 Eisenhower Avenue Alexandria, VA 22333	1	Commander US Army Electronics Research and Development Command Technical Support Activity ATTN: DELSD-L Fort Monmouth, NJ 07703
4	Commander US Army Armament Research and Development Command ATTN: DRDAR-TSS (2 cy) DRDAR-LCE, Dr. R.F.Walker DRDAT-LCE, Dr. N. Slagg Dover, ND 07801	3	Commander US Army Missile Command ATTN: DRSMI-R DRSMI-YDL DRSME-RK, Dr. R.G.Rhoades Redstone Arsenal, AL 35809
1	Commander US Army Armament Materiel Readiness Command ATTN: DRSAR-LEP-L, Tech Lib Rock Island, IL 62199	1	Commander US Army Tank Automotive Rsch and Development Command ATTN: DRDTA-UL Warren, MI 48090
1	Director US Army ARRADCOM Benet Weapons Laboratory ATTN: DRDAR-LCB-TL Watervliet, NY 12189	1	Director US Army TRADOC Systems Analysis Activity ATTN: ATAA-SL, Tech Lib White Sands Missile Range NM 88002
1	Commander US Army Aviation Research and Development Command ATTN: DRSAB-E 4300 Goodfellow Blvd. St. Louis, MO 63120	1	Commander US Army Research Office ATTN: Chemistry Division P.O. Box 12211 Research Triangle Park, NC 27709
1	Director US Army Air Mobility Research and Development Laboratory Ames Research Center Moffett Field, CA 94035	1	Commander Office of Naval Research ATTN: Dr. J. Enig, Code 200B 800 N. Quincy Street Arlington, VA 22217

DISTRIBUTION LIST

<u>No. of Copies</u>	<u>Organization</u>	<u>No. of Copies</u>	<u>Organization</u>
1	Commander Naval Sea Systems Command ATTN: Mr. R. Beauregard, SEA 64E Washington, DC 20362	1	Commander AFRPL ATTN: Mr. R. Geisler, Code AFRPL MKPA Edwards AFB, CA 93523
1	Commander Naval Explosive Ordnance Disposal Facility ATTN: Technical Library Code 604 Indian Head, MD 20640	1	Commander Ballistic Missile Defense Advanced Technology Center ATTN: Dr. David C. Sayles P.O. Box 1500 Huntsville, AL 35804
1	Commander Naval Research Lab ATTN: Code 6100 Washington, DC 20375	1	Director Lawrence Livermore National Lab University of California ATTN: Dr. M. Finger Livermore, CA 94550
1	Commander Naval Surface Weapons Center ATTN: Code G13 Dahlgren, VA 22448	1	Director Los Alamos National Lab ATTN: Dr. B. Craig, M Division P.O. Box 1663 Los Alamos, NM 87545
2	Commander Naval Surface Weapons Center ATTN: Mr. L. Roslund, Code R122 Mr. M. Stosz, Code R121 White Oak Lab Silver Spring, MD 20910	1	Schlumberger Well Services ATTN: Dr. C. Aseltine 5000 Gulf Freeway Houston, TX 77023
3	Commander Naval Weapons Center ATTN: Dr. L. Smith, Code 3205 Dr. A. Amster, Code 385 Dr. R. Reed, Jr., Code 388 China Lake, CA 93555		<u>Aberdeen Proving Ground</u> Dir, USAMSAA ATTN: DRXSY-D DRXY-MP, H. Cohen Cdr, USATECOM ATTN: DRSTE-TO-F Dir, USACSL, Bldg 3516, EA ATTN: DRDAR-CLB-PA
1	Commander Fleet Marine Force, Atlantic ATTN: G-4 (NSAP) Norfolk, VA 23511		

USER EVALUATION OF REPORT

Please take a few minutes to answer the questions below; tear out this sheet, fold as indicated, staple or tape closed, and place in the mail. Your comments will provide us with information for improving future reports.

1. BRL Report Number _____

2. Does this report satisfy a need? (Comment on purpose, related project, or other area of interest for which report will be used.)

3. How, specifically, is the report being used? (Information source, design data or procedure, management procedure, source of ideas, etc.) _____

4. Has the information in this report led to any quantitative savings as far as man-hours/contract dollars saved, operating costs avoided, efficiencies achieved, etc.? If so, please elaborate.

5. General Comments (Indicate what you think should be changed to make this report and future reports of this type more responsive to your needs, more usable, improve readability, etc.) _____

6. If you would like to be contacted by the personnel who prepared this report to raise specific questions or discuss the topic, please fill in the following information.

Name: _____

Telephone Number: _____

Organization Address: _____

----- FOLD HERE -----

Director
US Army Ballistic Research Laboratory
Aberdeen Proving Ground, MD 21005

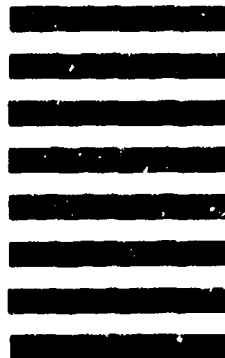


NO POSTAGE
NECESSARY
IF MAILED
IN THE
UNITED STATES

OFFICIAL BUSINESS
PENALTY FOR PRIVATE USE, \$300

BUSINESS REPLY MAIL
FIRST CLASS PERMIT NO 12062 WASHINGTON, DC
POSTAGE WILL BE PAID BY DEPARTMENT OF THE ARMY

Director
US Army Ballistic Research Laboratory
ATTN: DRDAR-TSB
Aberdeen Proving Ground, MD 21005



----- FOLD HERE -----